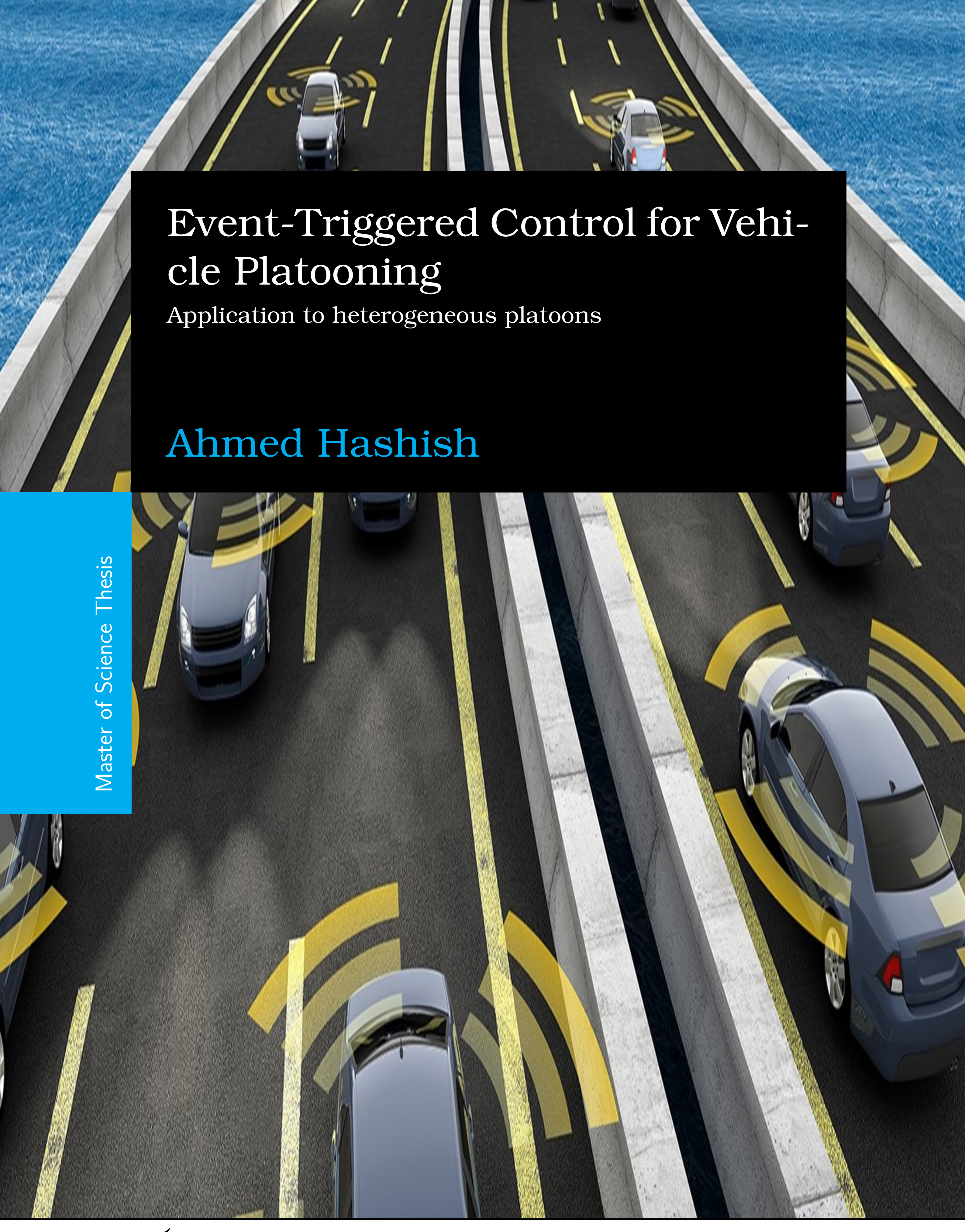

Event-Triggered Control for Vehicle Platooning

Application to heterogeneous platoons

Ahmed Hashish

Master of Science Thesis

Delft University of Technology

Delft Center for Systems and Control

Event-Triggered Control for Vehicle Platooning

Application to heterogeneous platoons

Master of Science Thesis

For the degree of Master of Science in Systems and Control at Delft University of Technology

Ahmed Hashish

November 29, 2018

Faculty of Mechanical, Maritime and Materials Engineering (3mE) · Delft University of Technology

Delft University of Technology
Department of
Delft Center for Systems and Control (dcsc)

The undersigned hereby certify that they have read and recommend to the Faculty of Mechanical, Maritime and Materials Engineering (3mE) for acceptance a thesis entitled

Event-Triggered Control for Vehicle Platooning

by

Ahmed Hashish

in partial fulfillment of the requirements for the degree of

Master of Science Systems and Control

Dated: November 29, 2018

Supervisor(s): ______________________
dr.ir. M. Mazo

____
Dr. A. Proskurnikov

Reader(s): ______________________
Dr.ir. R. Happee

____
Dr. R. Ferrari

Abstract

This thesis covers the implementation of Event-Triggering Control (ETC) on Cooperative Adaptive Cruise Control (CACC). CACC has the potential to increase road capacity, by having safe vehicle following with small intervehicle distance (less than 1 second), to increase traffic flow by eliminating shockwave effects, such that string-stable behavior is achieved, and it increases vehicle safety and driving comfort. CACC uses Vehicle-To-Vehicle (V2V) or Vehicle-To-Infrastructure (V2I) communication. However, excessive use of this wireless communication may result in reliability issues of the communication network. By means of Event-Triggered Control, this issue can be tackled by establishing communication only when it is necessary, while guaranteeing desired closed-loop performance.

In this thesis, an event-triggered controller for heterogeneous vehicle platooning is designed, which is decentralized, guarantees vehicle-following with small intervehicle distances, is robust against time-varying delays, and guarantees a positive minimum inter-event time. The algorithm is backed up by simulations, and it shows that communication is significantly reduced while maintaining desired closed-loop performance, when compared to periodic communication.

Table of Contents

Preface & Acknowledgements **ix**

1 Introduction **1**

1-1 Motivation for Cooperative Adaptive Cruise Control (CACC) 1

1-2 Necessity of Event-Triggered Control (ETC) 2

1-3 Current published work 3

1-4 Contribution and outline of the thesis 3

2 Notation and Definition **5**

2-1 Cooperative Adaptive Cruise Control 5

2-1-1 Introduction 5

2-1-2 Plant dynamics 6

2-1-3 Problem Formulation 7

3 Design of Event-Triggered Controllers for heterogeneous platoons **9**

3-1 Introduction 9

3-2 Design of the continuous-time controller 9

3-3 Design of the Event-Triggered Controller 10

3-4 Presence of communication delay 11

3-5 State-space of a heterogeneous pair of adjacent vehicles 11

3-6 The pair of adjacent vehicles modeled in presence of ETC and communication delay 12

3-7 $\mathcal{L}_2$-gain performance of the pair of adjacent vehicles 14

3-8 Guarantee of internal stability 14

4 Design of the controller in practice **15**

4-1 Introduction 15

4-2 Design of feedback controller and event-triggered controller 15

4-3 Determination of τ_{miet_i} and τ_{mad_i} 16

5 Simulation **17**
5-1 Introduction 17
5-2 Simulation results for different driving scenario's 18
5-2-1 Normal highway driving 18
5-2-2 Stop-And-Go 22
5-2-3 Emergency braking scenario 25

6 Conclusion **29**

A Preliminary mathematical notation **31**

B Design of Continuous Time CACC **33**
B-1 Introduction 33
B-2 The control law 33
B-3 Guarantee of internal vehicle stability 35

C Proof of Theorem 1 **39**

Bibliography **43**

Glossary **47**
List of Acronyms 47

List of Figures

1-1 Estimation of car sales from 2015 - 2040 1
1-2 Time Triggered Control (TTC) versus Event Triggered Control (ETC) 2
1-3 The event-triggering paradigm 2

2-1 A vehicle platoon 5

4-1 Determination of τ_{mad_i} and τ_{miet_i} 16

5-1 Velocity profile leader vehicle for normal highway driving 19
5-1 The simulation results for normal driving scenario 20
5-2 Velocity profile leader vehicle for stop-and-go scenario 22
5-2 The simulation results for stop-and-go scenario 24
5-3 Velocity profile leader vehicle for emergency braking scenario 25
5-3 The simulation results for emergency braking 27

List of Tables

5-1 Table listing all variables used for simulation 18

5-2 $\mathcal{L}_2$-norm of χ_i, e_i, defined over time $[0, 150]$ 21

5-3 Comparison of inter-transmission times between TTC and ETC for the vehicle platoons 22

5-4 $\mathcal{L}_2$-norm of χ_i, e_i, defined over time $[0, 150]$ 25

5-5 Comparison of inter-transmission times between TTC and ETC for the vehicle platoons 25

5-6 $\mathcal{L}_2$-norm of χ_i, e_i, defined over time $[0, 50]$ 27

5-7 Comparison of inter-transmission times between TTC and ETC for the vehicle platoons 28

Preface & Acknowledgements

I want to thank dr.ir. Manuel Mazo and Dr. Anton Proskurnikov for their support and valuable insights during the course of the thesis. Furthermore, I am very grateful for the unconditional support and love from family, friends and relatives, which kept me going to get the best out of myself.

The research was supported by NWO Domain TTW, The Netherlands, under the project TTW#13712 "From Individual Automated Vehicles to Cooperative Traffic Management - predicting the benefits of automated driving through on-road human behavior assessment and traffic flow models" (IAVTRM).

"The vehicles will be self-driving. So you have your own personal space where you can sit back and relax."

— *John Krafcik, CEO WAYMO*

Chapter 1

Introduction

1-1 Motivation for Cooperative Adaptive Cruise Control (CACC)

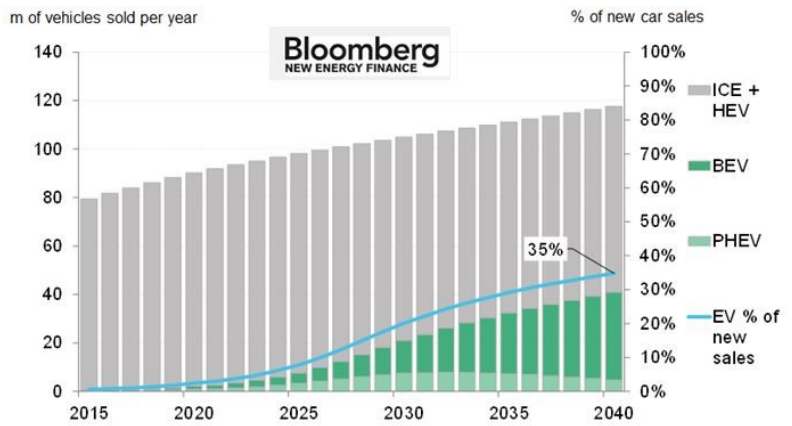

Figure 1-1: Estimation of car sales from 2015 - 2040. [1]

Traffic density is increasing due to the increasing number of vehicles on the road. Figure 1-1 shows the estimation of the number of car sales of the period 2015-2040 which can be observed to increase from approximately 80 million vehicles sold in 2015 to around 115 million sold in 2040 [1]. As the number of vehicles is increasing faster than the construction of public roads, it causes traffic congestion, longer traveling times, and more accidents. Most of these situations occur due to human handling, such as slow reaction times and bad decision making.

The desire is to increase road capacity, traffic throughput and make traveling safer and more comfortable. Automated driving is a promising technology for this. Cooperative Adaptive Cruise Control (CACC), which is part of automated driving, is a promising solution for this, which is an extension of the Adaptive Cruise Control (ACC) system. ACC keeps a certain desired speed while keeping a desired inter-vehicle distance to the predecessor vehicle. However, studies show that ACC cannot increase traffic throughput significantly with respect to manual driving. The additional Vehicle-to-Vehicle (V2V) and Vehicle-to-Infrastructure (V2I) communication gives more information to control the system, which gives the possibility to anticipate to the vehicle in front as opposed to reacting to a change of state of the leading vehicle. CACC has the potential to increase road capacity while maintaining a safe inter-vehicle distance, and increasing traffic flow by attenuating shockwave effects. [2]. This is all achieved by forming so-called vehicle strings or vehicle platoons, in which vehicles drive closely behind each other in the same lane. Additional advantages of platooning are the reduce of aerodynamic drag, resulting in lower fuel consumption, and enhanced safety and driving comfort [2] [3] [4].

1-2 Necessity of Event-Triggered Control (ETC)

Cooperative Adaptive Cruise Control (CACC) belongs to the group of networked control systems in which multiple agents collaborate to achieve a certain desired closed-loop performance. In case of CACC there is a wireless communication between vehicles (V2V) or between vehicles and infrastructure (V2I). Most CACC algorithms found in literature are continuous-time based [5, 6, 7, 8]. Implementation of these algorithms on a digital platform requires time sampling. The current paradigm used in digital control is the use of time-triggered control, in which the actuator is updated periodically. However, the choice of the sample time is not trivial. Generally, in engineering applications the sampling frequency is chosen to be at a high rate, usually as high as the digital platform allows. It could result in inefficient utilization of the available communication resources, which in case of CACC could result in inefficient utilization of the wireless communication, and possible reliability issues for the wireless communication network, due to excessive utilization.

Furthermore, it is more intuitive to update the controller when the system needs attention, for instance based on the system's state. This *event-triggered* scheduling paradigm results in more efficient utilization of the available communication resources while maintaining desired closed-loop performance. Furthermore, the vehicle's state is continuously monitored, which provides a high degree of robustness [9] [10] [11] [12].

Figure 1-2 shows the actuator scheduling time instants for both time-triggered and event-triggered control [3]. Furthermore, Figure 1-3 depicts the event-triggering paradigm.

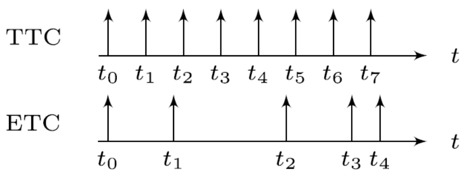

Figure 1-2: Time Triggered Control (TTC) versus Event Triggered Control (ETC) with respect to actuator update instants. [3]

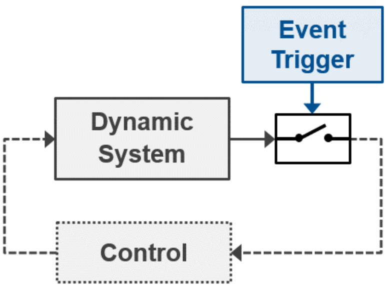

Figure 1-3: The event-triggering paradigm

Event-triggered control suffers from a couple of disadvantages with respect to time-triggered control. Firstly, the triggering system that detects when to close the loop must be monitored continuously real-time on the digital platform. Furthermore, the control output is updated aperiodically in event-triggered control, which could result in non-smooth actuation. Finally, a strictly positive dwell-time $\tau_{miet} = \inf_{k\geq 0}\{t_{k+1} - t_k\} > 0$ must be guaranteed in order to make it implementable on a digital platform.

1-3 Current published work

Challenges in designing controllers for vehicle platooning is to guarantee vehicle-following with small intervehicle distances, and guarantee attenuation of disturbances from head to tail. Furthermore, the desire is to design these controllers in a decentralized fashion. Next, since the controller will be implemented on a digital platform, it is subject to communication constraints. Overcoming this can be achieved using event-triggered control. The challenge in using event-triggered control is the guarantee of a strictly positive dwell-time, such that the time in between two sampling instants is lower-bounded by the dwell-time. Next, the desire is to design a decentralized triggering mechanism that preserves stability of the closed-loop system. An additional advantage of Event-Triggered Control is that it can be designed to trigger only whenever necessary, leading to efficient utilization of communication resource. Finally, communication networks suffer from delays, and the challenge is to preserve stability in presence of these delays.

Current work published on design of Event-Triggered Controller for vehicle platooning are few. [13] designs event-triggered controllers for vehicle platoons, which is decentralized and considers communication and actuator delay. By solving a set of Linear Matrix Inequalities (LMI's), internal stability and string stability are guaranteed, also in the presence of communication delays, and actuator delays. However, no guarantee on positive dwell-time is given.

[14] designs event-triggered controllers for vehicle platoons, using nonlinear vehicle dynamics, for general vehicle look-ahead topologies. The communication with neighboring vehicles is event-triggered and decentralized, and the vehicle's position and velocity are communicated. Due to the limited communication, this information is not continuously available. To overcome this, each vehicle estimates neighboring vehicles' position and velocity. The triggering rule is based on the difference between the estimate and the latest received measurement. Stability of the vehicle is guaranteed, but there is no guarantee of string stability. Furthermore, no communication delays are considered.

[3] published promising results, designing linear event-triggered controllers for homogeneous vehicle platoons, with decentralized controller structure, guaranteeing vehicle-following, and a relaxed form of string stability in the presence of communication delays.

1-4 Contribution and outline of the thesis

There is no current published work that designs Event-Triggered Controllers for general vehicle platoons, either homogeneous or heterogeneous, that is decentralized, event-triggered, guarantees vehicle following and string stability, and is robust against time-varying delays. The closest work that comes to satisfying all these requirements is [3]. Therefore, this thesis uses the steps and approach used in [3], and it is extended to a more general case. To be more concrete:

- An algorithm is proposed to design controllers for vehicles in vehicle platooning, which is decentralized and resource-aware, robust against time-varying delays, and guarantees vehicle following and a relaxed form of string stability. This is done in the following steps:
  - A decentralized controller is designed to guarantee vehicle following. This is designed in continuous time, and therefore not yet resource-aware.
  - The controller is made resource-aware by designing an Event-Triggered Controller, which determines when to transmit a new measurement to a successor vehicle, while guaranteeing a relaxed form of string stability. Part of the design is based on finding a solution for an optimization problem, containing Linear Matrix Inequalities.
  - Robustness against time-varying delays is guaranteed by showing a non-increase of a storage function. The same principle is used to guarantee a strictly positive dwell-time.
- The algorithm is tested by simulation to test the performance of the vehicle platoon under event-triggered communication and communication delays. It is compared to a more conventional paradigm, periodic control, in terms of closed-loop performance, and the amount of communication. This is tested for different driving scenario's:
  - Normal highway driving with gentle accelerations and decelerations of the platoon leader.
  - Stop-and-go driving by the platoon leader such as in traffic congestions.
  - Emergency braking by the platoon leader, e.g. for a sudden obstacle on the road.

Outline

The chapters outlined in the thesis guide the reader through the step-by-step approach to design such controllers.

In Chapter 2, preliminary information is given on the notation for CACC used throughout the thesis. This consists of the used plant dynamics, controller structure, spacing topology, and the problem formulation.

In Chapter 3 the Event-Triggered Controller is designed. In this chapter a relaxed form of string stability and guaranteed internal stability in presence of event-triggered control and time-varying delays is also guaranteed.

In Chapter 4 a recipe is given how to design a controller for vehicle platooning, how to determine the dwell-time, and how to find an upper-bound on the time-varying delays for which stability is preserved, and some recommendations on how to tune.

Chapter 5 carries out simulations to put the controller designed in Chapter 4 into practice for the above-mentioned driving scenario's.

Finally, a conclusion is given in Chapter 6.

Chapter 2

Notation and Definition

2-1 Cooperative Adaptive Cruise Control

2-1-1 Introduction

Consider Figure 2-1, representing a vehicle platoon.

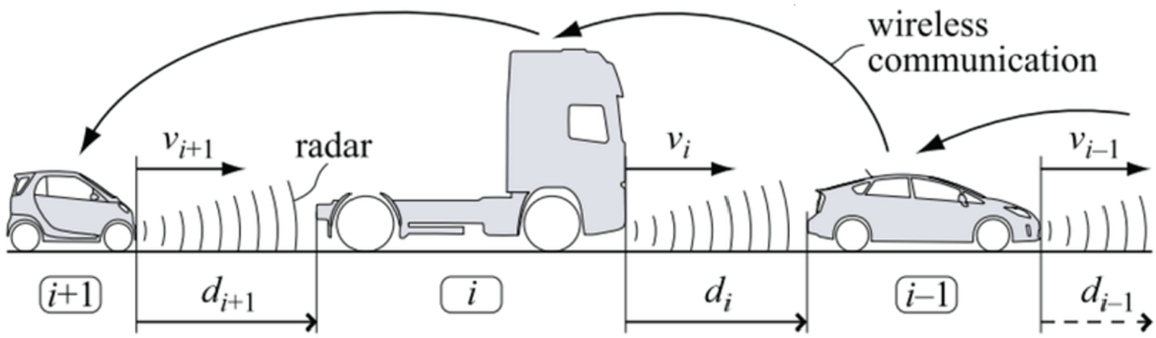

Figure 2-1: A vehicle platoon consisting of non-identical vehicles. All vehicles are equipped with a speed sensor measuring the vehicle speed v_i, a radar measuring the intervehicle distance d_i, sensor to measure the vehicle's acceleration, and hardware to communicate with a following vehicle. [8]

Figure 2-1 represents a vehicle platoon. Each vehicle in the vehicle string is equipped with the hardware necessary for CACC, i.e. a radar/lidar to measure intervehicle distance d_i, a speed sensor to measure v_i, an acceleration sensor to measure a_i, and hardware to establish communication over a wireless network with the first successor vehicle. Furthermore, it is assumed that no packet losses occur, which means all transmitted data is successfully received by the succeeding vehicle. In Figure 2-1 there is a one vehicle look-ahead communication topology being used, in which there is vehicle communication only with the first successor vehicle. This is the only communication topology considered throughout this report. Other possible communication topologies are bidirectional topology or two-vehicle look-ahead topology or communication with the leader [15].

2-1-2 Plant dynamics

The intervehicle distance d_i is defined as:

$$d_i(t) := q_{i-1}(t) - q_i(t), \quad i = 1...N \tag{2-1}$$

with q_{i-1} the position of vehicle $i-1$, and q_i the position of vehicle i.

The goal of each vehicle is to follow the predecessor vehicle with a certain desired intervehicle distance, which is denoted by $d_{r,i}$. The spacing policy used for this is the constant time-headway spacing policy.

$$d_{r,i}(t) := d_{0_i} + h_i v_i(t), \quad i = 1...N \tag{2-2}$$

with d_{0_i} defined as the standstill distance, h_i defined as the time headway, i.e. the number of seconds to the predecessor, and v_i the speed of vehicle i.

The difference between the actual intervehicle distance and the desired intervehicle distance is defined as the spacing error e_i.

$$e_i(t) := d_i(t) - d_{r,i}(t), \quad i = 1...N \tag{2-3}$$

The vehicle dynamics considered for the longitudinal motion of vehicle i are defined in Eq. (2-4). This model is not trivial at first sight. It is a third-order linear model extended with controller dynamics u_i, whose derivation can be found in Appendix B.

$$\begin{pmatrix} \dot{e}_i(t) \\ \dot{v}_i(t) \\ \dot{a}_i(t) \\ \dot{u}_i(t) \end{pmatrix} = \left(\begin{array}{c} v_{i-1}(t) - v_i(t) - h_i a_i(t) \\ a_i(t) \\ -\frac{1}{\tau_{d_i}} a_i(t) + \frac{1}{\tau_{d_i}} u_i(t) \\ \hline O_i Q_i a_i(t) - O_i R_i u_i(t) + O_i \chi_i(t) \end{array} \right), \quad i = 1...N \tag{2-4}$$

with e_i the spacing error, v_i the vehicle velocity, a_i the actual acceleration, u_i the input into the vehicle driveline, χ_i the controller output, and $\tau_{d_i} \in \mathbb{R}_{>0}$ a time constant representing driveline dynamics. O_i, Q_i, R_i are defined as in Eq. (2-5)-(2-7)

$$O_i = \frac{\tau_{d_i}}{h_i \tau_{d_{i-1}}} \tag{2-5}$$

$$Q_i = -1 + \frac{\tau_{d_{i-1}}}{\tau_{d_i}} - \frac{h_i \tau_{d_{i-1}}}{\tau_{d_i^2}} + \frac{h_i}{\tau_{d_i}} \tag{2-6}$$

$$R_i = \frac{\tau_{d_{i-1}}}{\tau_{d_i}} - \frac{h_i \tau_{d_{i-1}}}{\tau_{d_i}^2} + \frac{h_i}{\tau_{d_i}} \tag{2-7}$$

The third-order model is adopted from [7], and the derivation of the third-order model from a more detailed nonlinear model can be found in [16, 17]. The extension to Eq. (2-4) is given in Appendix B.

Next, the problem that is addressed in this thesis is formulated.

2-1-3 Problem Formulation

A well-designed CACC guarantees that each individual vehicle is internally stable, and that the vehicle platoon is string stable. The following problem statement is formulated, which gives properties to satisfy internal vehicle stability and string stability.

Problem 1. *Consider the vehicle platoon depicted in Figure 2-1, with the dynamics for each vehicle defined by Eq. (2-4). Then for a well-designed CACC, each individual vehicle and the entire platoon must comply with the following two things:*

- *Internal vehicle stability: For each vehicle i it must hold that if, $v_0(t) = v_c$, with v_c a constant velocity, $\forall t \in \mathbb{R}_{\geq 0}$, then*

$$\lim_{t\to\infty} e_i(t) = 0, \lim_{t\to\infty} v_i(t) = v_c, \lim_{t\to\infty} u_i(t) = 0 \quad \forall i = 1...N \tag{2-8}$$

- *Relaxed String stability: The disturbances are not amplified as they propagate through the platoon in the sense that [3, 7, 8]*

$$||\chi_i||_{\mathcal{L}_2} \leq \alpha_i||\chi_{i-1}||_{\mathcal{L}_2} + \beta_i(||x_i(0)||) \quad \forall i = 1...N \tag{2-9}$$

with α_i a nonnegative constant, β_i a $\mathcal{K}_\infty$-function[1]*, and $x_i(0)$ the initial condition.*

These two conditions must hold in presence of communication delays and it must hold when data transmissions are significantly reduced to only when necessary.

In Eq. (2-9) accelerations are used for the $\mathcal{L}_2$-gain analysis, which is adopted from [3]. Due to the communication topology that is used, and using this property, a state-space formulation that analyzes the $\mathcal{L}_2$-gain from χ_{i-1} to χ_i can be realized that is not affected by other vehicles, and gives an overlapping decomposition of the entire platoon, making the state dimension small and, therefore, computationally tractable. Other variables that may be used for the string-stability analysis are attenuation of the spacing error e_i, actual acceleration a_i, or velocity v_i. Examples of other papers using this definition can be found in [7, 8, 18, 19]. Guaranteeing performance in terms of $\mathcal{L}_2$ is chosen for Eq. (2-9), because the $\mathcal{L}_2$-gain of a linear time-invariant dynamical system in the time-domain is equivalent to the $\mathcal{H}_\infty$-norm of a linear time-invariant system in the frequency domain [20].

[1]See Appendix A for the definition of a $\mathcal{K}_\infty$ function

Chapter 3

Design of Event-Triggered Controllers for heterogeneous platoons

3-1 Introduction

In this chapter, the controller is designed for vehicles in a vehicle platoon, which determines when to communicate with the successor vehicle, and has guaranteed $\mathcal{L}_2$-gain performance and internal stability. Firstly, the controller is designed in continuous-time. Then, an Event-Triggered Controller is designed to make the continuous-time controller sampled and applicable on a digital platform. Next, a pair of adjacent vehicles is modeled in presence of the Event-Triggered Controller and communication delay. Finally, finite $\mathcal{L}_2$-gain performance of a pair of adjacent vehicles and internal stability of an individual vehicle is guaranteed.

3-2 Design of the continuous-time controller

This section covers the design of the continuous-time controller, which includes the structure of χ_i and guarantee of internal vehicle stability. This design also serves as a preliminary recommendation on how to design continuous-time CACC controllers. The derivation can also be found in Appendix B.

Consider Eq. (2-4), which are the plant dynamics used for the controller design. The structure of χ_i is chosen such that it stabilizes the error dynamics $e_i, \dot{e}_i, \ddot{e}_i$ by means of a feedback controller, with $k_{p_i}, k_{d_i}, k_{dd_i}$ gains on the errors respectively, and simultaneously compensates for the term u_{i-1}, which is acquired through wireless communication with the predecessor vehicle. For this reason, χ_i consists of a local feedback controller, and a feedforward part.

$$\chi_i(t) = k_{p_i} e_i(t) + k_{d_i} \dot{e}_i(t) + k_{dd_i} \ddot{e}_i(t) + u_{i-1}(t) \tag{3-1}$$

In order to guarantee internal vehicle stability, the gains $k_{p_i}, k_{d_i}, k_{dd_i}$ must be chosen such that Lemma 2 holds, i.e.

$$(1 + k_{dd_i})\, k_{d_i} - k_{p_i} \tau_{d_{i-1}} > 0 \tag{3-2}$$

with $h_i, \tau_{d_{i-1}}, \tau_{d_i}, k_{p_i}, k_{d_i} > 0, k_{dd_i} > -1$. The proof of this Lemma is given in Appendix B, to guarantee asymptotic stability of the error dynamics $e_i, \dot{e}_i, \ddot{e}_i$.

For the remainder of the thesis, it is assumed that $k_{dd_i} = 0$, as this is a gain on $\ddot{e}_i$. $\ddot{e}_i$ depends on the vehicle jerk, which cannot be obtained from sensor data, such that

$$\chi_i(t) = k_{p_i} e_i(t) + k_{d_i} \dot{e}_i(t) + u_{i-1}(t) \tag{3-3}$$

3-3 Design of the Event-Triggered Controller

Consider Eq. (3-3), the definition of χ_i. It is assumed that the term u_{i-1} is continuously available, which in practice does not hold. In reality, this term is transmitted at time instants $t_k^i, \quad k \in \mathbb{N}_{\geq 0}$. As such, χ_i becomes

$$\chi_i(t) = k_{p_i} e_i(t) + k_{d_i} \dot{e}_i(t) + \hat{u}_{i-1}(t) \tag{3-4}$$

with $\hat{u}_{i-1}$ the latest received measurement from vehicle i. The feedback controller remains continuous under the assumption that a much higher frequency (100 Hz) is used for local sensor data [3, 19]. To make $\hat{u}_i$ sampled, an event-triggered controller is designed, which determines when to transmit a new measurement to the following vehicle. By means of the Event-Triggered Controller, a messaging scheduler is designed, which is sampled and makes this controller implementable on digital platforms.

The network-induced error is defined below.

$$e_{u_i}(t) = \hat{u}_i(t) - u_i(t), \quad i = 0...N-1 \tag{3-5}$$

with $\hat{u}_i$ the latest transmitted measurement of u_i, and u_i its current value.

In order to make the event-triggering controller decentralized, each vehicle determines individually when to transmit a new measurement. Furthermore, the mechanism for each vehicle must only consist of local variables, i.e. only variables that are accessible to the vehicle, e.g. u_i, χ_i, a_i. Therefore, the event-triggering mechanism is defined below, which determines when to transmit a new measurement of u_i from vehicle i to vehicle $i+1$.

$$t_{k+1}^i := \inf\{t > t_k^i + \tau_{miet_i} | \eta_i(t) \leq 0\}, \quad t_0^i = 0, \quad k \in \mathbb{N}_{\geq 0}, \quad \forall i = 0...N-1 \tag{3-6}$$

$$\dot{\eta}_i(t) := \varrho_i u_i^2 + \omega(\tau_i)\left((1-\varepsilon_i) O_i^2 |R_i u_i - \chi_i - Q_i a_i|^2 - \gamma_i^2 \left(1 + \frac{1}{\varepsilon_i}\phi_{i,0}^2(\tau_{miet})\right) e_{u_i}^2\right) \tag{3-7}$$

$$\hat{u}_i(t) = \begin{cases} u_i(t_k^i), & \text{when } \eta_i(t) \leq 0 \\ \hat{u}_i(t_k^i), & \text{when } \eta_i(t) > 0 \end{cases} \tag{3-8}$$

with O_i, R_i, Q_i defined in Eq. (2-5)-(2-7), $\varrho_i, \varepsilon_i \in \mathbb{R}_{\geq 0}$ tuning variables, $\omega(\tau_i)$ a logic variable as defined in Eq. (3-10), $\phi_{l_i}(\tau_i)$ defined in Eq. (3-9),

$$\begin{aligned} \dot{\phi}_{i,l_i}(\tau_i) &= -(1-\omega(\tau_i))\gamma_{i,l_i}(\phi_{i,l_i}^2(\tau_i) + 1), \quad l_i \in \{0,1\} \\ \gamma_{i,0} &:= \gamma_i, \quad \gamma_{i,1} := \frac{\gamma_i}{\lambda_i}, \quad \lambda_i \in (0,1) \ (\lambda_i: \text{ A tuning parameter}) \end{aligned} \tag{3-9}$$

$$\omega(\tau_i) = \begin{cases} 0, & \tau_i \leq \tau_{miet} \\ 1, & \tau_i > \tau_{miet} \end{cases} \tag{3-10}$$

$\tau_{miet} \in \mathbb{R}_{>0}$ the minimum inter-event times, and τ_i a timer that keeps track on the time elapsed since the latest measurement.

The event-triggering variable η_i evolves continuously and its derivative changes based on Eq. (3-7). Such an event-triggering variable is called a *dynamic event-generator*, which has the advantage over a static event-generator that it results in larger inter-event times. This dynamic event-generator is proposed in [21].

3-4 Presence of communication delay

Communication networks in general suffer from communication delays. Therefore, the communication delay is taken into account in the design of the Event-Triggered Controller. The communication delay is defined as $\Delta_k^i, k \in \mathbb{N}$. This means that when a new transmission of u_i is scheduled at time t_k^i, it gets received and updated by the following vehicle at time $t_k^i + \Delta_k^i$, such that

$$\hat{u}_i((t_k^i + \Delta_k^i)^+) = u_i(t_k^i) \tag{3-11}$$

In between two events, $\hat{u}_i$ is kept constant, such that the following assumption is adopted.

$$\dot{\hat{u}}_i(t) = 0, \quad \forall t \in (t_k^i + \Delta_k^i, t_{k+1}^i + \Delta_{k+1}^i), \quad k \in \mathbb{N}, \quad \forall i = 0...N-1 \tag{3-12}$$

Finally, it is assumed that the communication delay Δ_k^i is upper bounded by a maximum allowable delay τ_{mad_i}. Furthermore, it is assumed a new transmission can only be scheduled if the previous instant is received by the following vehicle.

Assumption 1. *The communication delay is bounded according to*

$$0 \leq \Delta_k^i \leq \tau_{mad_i} \leq \tau_{miet_i}, \quad k \in \mathbb{N}, \quad \forall i = 0...N-1 \tag{3-13}$$

with $\tau_{mad_i} \in \mathbb{R}_{\geq 0}$ the maximum allowable delay. This is a requirement on the choice of parameters.

3-5 State-space of a heterogeneous pair of adjacent vehicles

As stated in Eq. (2-9), we aim to evaluate a relaxed form of string stability in the presence of network-induced errors by analyzing the $\mathcal{L}_2$-gain with respect to χ_i as input and χ_{i+1} as output. To do that, a state-space is formulated, which models a pair of adjacent vehicles.

The lumped state vector is defined as

$$\tilde{x}_i := \begin{bmatrix} v_i & a_i & u_i & e_{i+1} & v_{i+1} & a_{i+1} & u_{i+1} \end{bmatrix}^T \quad i = 0...N-1 \tag{3-14}$$

Then, using Eq. (2-4) and Eq. (3-4), the following state-space model can be derived.

$$\dot{\tilde{x}}_i(t) = A_i\tilde{x}_i(t) + B_i\chi_i(t) + E_i\hat{u}_i(t) \tag{3-15}$$

$$A_i = \begin{pmatrix} 0 & 1 & 0 & 0 & 0 & 0 & 0 \\ 0 & -\frac{1}{\tau_{d_i}} & \frac{1}{\tau_{d_i}} & 0 & 0 & 0 & 0 \\ 0 & O_iQ_i & -O_iR_i & 0 & 0 & 0 & 0 \\ 1 & 0 & 0 & 0 & -1 & -h_{i+1} & 0 \\ 0 & 0 & 0 & 0 & 0 & 1 & 0 \\ 0 & 0 & 0 & 0 & 0 & -\frac{1}{\tau_{d_{i+1}}} & \frac{1}{\tau_{d_{i+1}}} \\ k_{d_{i+1}}O_{i+1} & 0 & 0 & k_{p_{i+1}}O_{i+1} & -k_{d_{i+1}}O_{i+1} & O_{i+1}\left(Q_{i+1} - k_{d_{i+1}}h_{i+1}\right) & -O_{i+1}R_{i+1} \end{pmatrix} \tag{3-16}$$

$$B_i = \begin{pmatrix} 0 & 0 & O_i & 0 & 0 & 0 & 0 \end{pmatrix}^T \tag{3-17}$$

$$E_i = \begin{pmatrix} 0 & 0 & 0 & 0 & 0 & 0 & O_{i+1} \end{pmatrix}^T \tag{3-18}$$

with O_i, Q_i, R_i as in Eq. (2-5)-(2-7). It is assumed that the value of $\tau_{d_{i+1}}$ is known to vehicle i.

This formulation gives an overlapping decomposition from two consecutive vehicles of the vehicle platoon, which can be any two types of vehicles, depending on the value of τ_{d_i} and $\tau_{d_{i+1}}$ respectively. If it can be shown that if this subsystem has a finite $\mathcal{L}_2$-gain, then it can be shown that vehicle $i+1$'s $\chi_{i+1} \in \mathcal{L}_2$ if $\chi_i \in \mathcal{L}_2$.

3-6 The pair of adjacent vehicles modeled in presence of ETC and communication delay

In this section, Section 3-4 and Section 3-5 are combined into one model describing a pair of adjacent vehicles. Next, this model is used for the $\mathcal{L}_2$-gain performance of a pair of adjacent vehicles.

For the pair of adjacent vehicles, there are three cases that are considered. The first case is when vehicle i sends a new measurement. This resets the local timer τ_i used in Eq. (3-7) and Eq. (3-10), and the network induced error e_{u_i} as defined in Eq. (3-5).

The second case is due to the communication delay, as can be seen in Eq. (3-11). This occurs when a new measurement of $\hat{u}_i$ is received by the following vehicle, which updates the controller χ_{i+1}. In presence of communication delay, the transmission of a new measurement by vehicle i and the update of that measurement by vehicle $i+1$ does not happen simultaneously. Finally, the third situation, is when no transmission or update occurs.

This addition reformulates the state-space of Eq. (3-15) to Eq. (3-21)-Eq. (3-22). The three cases are distinguished as follows: 1) when vehicle i transmits a new measurement, 2) when vehicle $i+1$ receives the new measurement, 3) the pair of adjacent vehicles in between events.

$$\xi^+_{i,(1)} = \begin{pmatrix} \tilde{x}^+_i \\ e^+_{u_i} \\ \tau^+_i \\ \eta^+_i \end{pmatrix} = \begin{pmatrix} \tilde{x}_i \\ 0 \\ 0 \\ \eta_i \end{pmatrix} \tag{3-19}$$

$$\xi^+_{i,(2)} = \begin{pmatrix} \tilde{x}^+_i \\ e^+_{u_i} \\ \tau^+_i \\ \eta^+_i \end{pmatrix} = \begin{pmatrix} \tilde{x}_i \\ e_{u_i} \\ \tau_i \\ \eta_i \end{pmatrix} \tag{3-20}$$

$$\dot{\xi}_i = \begin{pmatrix} \dot{\tilde{x}}_i \\ \dot{e}_{u_i} \\ \dot{\tau}_i \\ \dot{\eta}_i \end{pmatrix} = \begin{pmatrix} A_{11_i}\tilde{x}_i + A_{12_i}e_{u_i} + A_{13_i}\chi_i \\ O_i\left(R_iu_i - \chi_i - Q_ia_i\right) \\ 1 \\ \varrho_iu_i^2 + \omega(\tau_i)\left(\left(1-\varepsilon_i\right)O_i^2\left(R_iu_i - \chi_i - Q_ia_i\right)^2 - \gamma_i^2\left(1 + \frac{1}{\varepsilon_i}\phi(\tau_{mieti})\right)e^2_{u_i}\right) \end{pmatrix} \tag{3-21}$$

$$\chi_{i+1} = C_{z_i}\tilde{x}_i + D_{z_i}e_{u_i} \quad \text{(Performance output)} \tag{3-22}$$

with $e_{u_i} = \hat{u}_i - u_i$, τ_i the local timer which keeps track of the time elapsed since the latest transmission, $\varepsilon_i \in (0,1)$ a tuning parameter, $\varrho \in \mathbb{R}_{\geq 0}$ a tuning parameter, $\gamma \in \mathbb{R}_{>0}$ a solution to a matrix inequality given in Eq. (3-30). O_i, R_i, Q_i are defined in Eq. (2-5)- (2-7), and $\phi_i, \omega(\tau_i)$ defined in Eq. (3-9), and Eq. (3-10).

Finally,

$$A_{11_i} = A_i + E_iC_1 \tag{3-23}$$
$$A_{12_i} = E_i \tag{3-24}$$
$$A_{13_i} = B_i \tag{3-25}$$
$$u_i = C_1\tilde{x}_i \tag{3-26}$$
$$a_i = C_2\tilde{x}_i \tag{3-27}$$

with A_i, B_i, E_i defined as in Eq. (3-16)-Eq. (3-18), $C_1 = \begin{pmatrix} 0 & 0 & 1 & 0 & 0 & 0 & 0 \end{pmatrix}$ and, $C_2 = \begin{pmatrix} 0 & 1 & 0 & 0 & 0 & 0 & 0 \end{pmatrix}$

$$C_{z_i} = \begin{pmatrix} k_{d_{i+1}} & 0 & 1 & k_{p_{i+1}} & -k_{d_{i+1}} & -k_{d_{i+1}}h_{i+1} & 0 \end{pmatrix} \tag{3-28}$$
$$D_{z_i} = 1 \tag{3-29}$$

3-7 $\mathcal{L}_2$-gain performance of the pair of adjacent vehicles

Theorem 1. *Consider the pair of adjacent vehicles formulated by Eq. (3-19)-Eq. (3-22). Then there exists* $\gamma_i, \mu_i \in \mathbb{R}_{>0}$, $P_i = P_i^T \succeq 0$ *such that* $M_i \preceq 0$ *holds, with* M_i *equal to*

$$M_i = \begin{pmatrix} M_1 & P_i A_{12_i} + \mu_i C_{z_i}^T D_{z_i} & P_i A_{13_i} - O_i^2 G_1^T \\ A_{12_i}^T P_i + \mu_i D_{z_i}^T C_{z_i} & \mu_i D_{z_i}^T D_{z_i} - \gamma_i^2 & 0 \\ A_{13_i}^T P_i - O_i^2 G_1 & 0 & O_i^2 - \mu_i(1+\epsilon_i) \end{pmatrix} \tag{3-30}$$

$$M_1 = A_{11_i}^T P_i + P_i A_{11_i} + \mu_i C_{z_i}^T C_{z_i} + \varrho_i C_1^T C_1 + O_i^2 G_1^T G_1$$

$$G_1 = (R_i C_1 - Q_i C_2)$$

and $\tau_{mad_i} \in \mathbb{R}_{\geq 0}, \tau_{miet_i} \in \mathbb{R}_{>0}$, *with* $\tau_{mad_i} \leq \tau_{miet_i}$, *such that the system given in Eq. (3-19)-Eq. (3-22) has a finite* $\mathcal{L}_2$*-gain not greater than* $\sqrt{1+\epsilon_i}, \epsilon_i \in \mathbb{R}_{\geq 0}$, *with respect to* χ_i *as input and* χ_{i+1} *as output.*

The proof is given in Appendix C.

Showing this guarantees the relaxed string-stability condition for a pair of adjacent vehicles defined in Eq. (2-9). String-stability can be guaranteed for $\epsilon_i = 0, \quad \forall i = 0...N-1$. Although this is usually not found in experiments, ϵ_i can often be chosen small, which guarantees almost string-stability.

3-8 Guarantee of internal stability

Finally, convergence of the spacing error e_i needs to be guaranteed, which is proven in the following lemma.

Lemma 1. *Consider the system defined by Eq. (2-4), and assuming the conditions from Theorem 1 hold. Furthermore, assume that the leader vehicle drives with constant speed,* $v_0 = v_c$, *with* v_c *a constant velocity. Then,* $e_i \to 0$.

Proof. Firstly, we use the assumption that the condition from Theorem 1 holds, such that if $\chi_{i-1} \in \mathcal{L}_2$, then $\chi_i \in \mathcal{L}_2$. Next, consider the matrix Z_i given in Eq. (B-14), which is the closed-loop form of the system. It already contains χ_i in the form of k_{p_i} and k_{d_i}. Under the condition that k_{p_i}, k_{d_i} are chosen in accordance with Lemma 2 and Eq. (3-2), the matrix Z_i in Eq. (B-14) is asymptotically stable. Since $\chi_i \in \mathcal{L}_2$, and Z_i is asymptotically stable, $e_{1_i}, e_{2_i}, e_{3_i} \in \mathcal{L}_2$. Recall the definition for $e_{1_i}, e_{2_i}, e_{3_i}$ from Eq. (B-2), i.e. $e_{1_i} = e_i, e_{2_i} = \dot{e}_i, e_{3_i} = \ddot{e}_i$. Therefore, since $e_i, \dot{e}_i, \ddot{e}_i \in \mathcal{L}_2$, it can be concluded using Barbalat's Lemma, that $e_i \to 0$. [22] □

Chapter 4

Design of the controller in practice

4-1 Introduction

In this chapter, it is explained how to design the feedback controller and the Event-Triggered Controller.

4-2 Design of feedback controller and event-triggered controller

We start with the design of the feedback controller. The gains k_{p_i}, and k_{d_i} are chosen such that Lemma 2 holds. Next, the Event-Triggered Controller is designed, which is given in Eq. (3-7). For this, the parameters γ_i and τ_{miet_i} are needed. $\gamma_i \in \mathbb{R}_{>0}$ is a solution for which the matrix inequality $M_i \preceq 0$ holds, with M_i as in Eq. (3-30).

The design of the controller is set as an optimization problem in which γ_i is minimized, which is done to maximize the value of τ_{miet_i}.

$$\begin{aligned} \min \quad & \gamma_i & \text{(4-1)} \\ \text{s.t} \quad & M_i \preceq 0 \quad i = 0...N-1 \\ & P_i = P_i^T \succeq 0 \\ & k_{d_i} - k_{p_i}\tau_{d_{i-1}} > 0 & \text{(4-2)} \end{aligned}$$

When trying to find a solution to the optimization problem, we tend to keep ϵ_i low as we want to keep the $\mathcal{L}_2$-gain low, but on the other hand this may result in a large value for γ_i, which results in a small value for τ_{miet_i}. Therefore, a trade-off needs to be found. Simulations suggest that through trial-and-error, $\gamma < 10$ is a good value for the event-triggered controller.

Furthermore, finding a solution for Eq. (4-1) for $\epsilon_i = 0$ cannot be found for all vehicles. This implies that string-stability cannot be guaranteed from the algorithm.

Finally, tuning parameters such as $\varrho_i \in \mathbb{R}_{\geq 0}$, and $\varepsilon_i \in (0, 1)$, are used in the optimization problem in Eq. (4-1), and in the Event-Triggered Controller in Eq. (3-7).

The optimization problem posed in Eq. (4-1) can be solved using online solvers. The solver used here is the SeDuMi solver [23] together with the yalmip interface [24].

Next step in the design of the controller, is the determination of the time constants τ_{mad_i} and τ_{miet}.

4-3 Determination of τ_{miet_i} and τ_{mad_i}

For the determination of the time constants, we make use of Theorem 1, in particular Eq. (C-14) and Eq. (C-15). We determine τ_{miet_i} and $\tau_{mad_i}, \quad i = 0...N-1$ such that these inequalities hold, which is outlined below.

$$\tau_{mad_i} = \inf\{0 \leq \tau_i \leq \tau_{mad_i} | \gamma_{i,0}\phi_{i,0}(\tau_i) \leq \gamma_{i,1}\phi_{i,1}(\tau_i)\} \tag{4-3}$$

$$\tau_{miet_i} = \inf\{\tau_i \geq \tau_{mad_i} | \gamma_{i,0}\phi_{i,0}(\tau_i) \geq 0\} \tag{4-4}$$

with γ_i the solution of the optimization problem in Eq. (4-1), and $\gamma_{i,0}, \gamma_{i,1}$ defined in Eq. (3-9), and $\phi_{i,l_i}(\tau_i),\ l_i \in \{0,1\}$ defined in Eq. (3-9). It is crucial that $\tau_{miet_i} \geq \tau_{mad_i}$ to not violate Assumption 1. The initial conditions of $\phi_{i,0}$ and $\phi_{i,1}$ must be chosen such that the inequalities in Eq. (4-3) and Eq. (4-4) hold, such that $\phi_{i,0}(0) \geq 0$, and $\phi_{i,1}(0) \geq \dfrac{\gamma_{i,0}\phi_{i,0}(0)}{\gamma_{i,1}}$.

In practice, a lower value for λ_i, results in a higher value for τ_{miet_i} and a lower value for τ_{mad_i}, such that lowering λ_i lets these variables go further away from each other. A larger value for λ_i brings these variables closer to each other. Increasing or decreasing of λ_i can be done up to a certain point. Lowering can be done as long as no discontinuities appear in one of the design functions (See Figure 4-1 for the functions), which may happen for the function $\gamma_{i,1}\phi_{i,1}(\tau_i)$. Next, increasing λ_i can be done as long as the condition $\tau_{mad_i} \leq \tau_{miet_i}$ holds.

An example of how τ_{mad_i} and τ_{miet_i} are determined in practice is depicted in Figure 4-1.

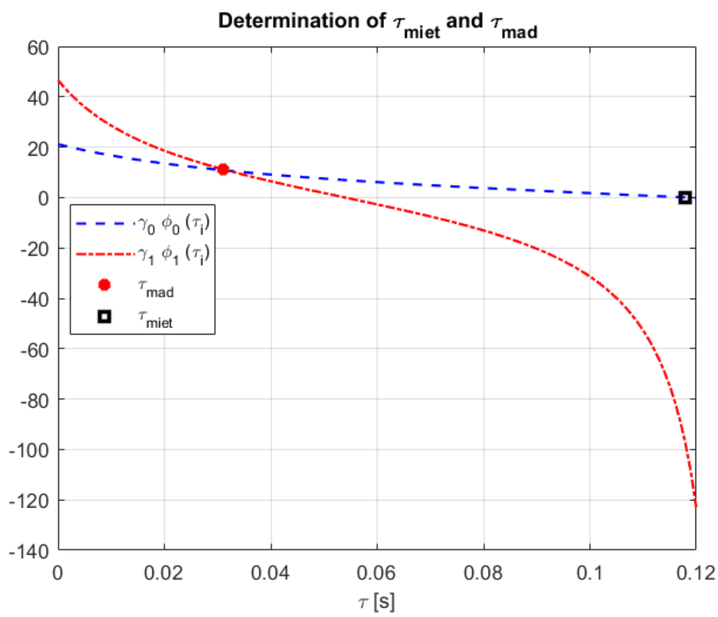

Figure 4-1: Determination of τ_{mad_i} and τ_{miet_i}

Chapter 5

Simulation

5-1 Introduction

In this Chapter, simulations are carried out to evaluate vehicle platoons with event-triggered controllers for a heterogeneous platoon, using the recipe given in Chapter 4. The vehicle platoon is tested for three different driving scenario's: normal highway driving, stop-and-go driving, and emergency braking. [25].

A heterogeneous platoon of six vehicles is considered in the simulation. Table 5-1 displays the parameters for the design of the event-triggered control and the simulation.

Each vehicle knows his own parameter time constant, i.e. τ_{d_i}, and the time constant $\tau_{d_{i-1}}$ of the predecessor vehicle, and the time constant $\tau_{d_{i+1}}$ of the successor vehicle.

The gains k_{p_i} and $k_{d_i}, \quad i = 1...3$ are chosen such that they comply with Lemma 2. The solution to the optimization problem given in Eq. (4-1) is given below with their respective tuning parameters ϱ and ϵ. Finally, the values of τ_{mad_i} and τ_{miet_i} are determined according to Eq. (4-3) and Eq. (4-4). The initial conditions used for $\phi_{i,l_i}, \quad i = 1...5, l_i \in \{0, 1\}$ are $\phi_{i,0}(0) = \dfrac{1}{\lambda_i}$, $\phi_{i,1}(0) = \dfrac{\gamma_{i,0}\phi_{i,0}(0)}{\gamma_{i,0}\lambda_i}$.

Table 5-1: Table listing all variables used for simulation

Variable (unit)	Vehicle 1	Vehicle 2	Vehicle 3	vehicle 4	vehicle 5	vehicle 6
τ_{d_i} (s)	0.1	1	0.5	0.8	0.3	1
h_i (s)	0.6	0.6	0.6	0.6	0.6	0.6
k_{p_i}	0.2	0.2	0.2	0.2	0.2	0.2
k_{d_i}	0.7	0.7	0.7	0.7	0.7	0.7
d_{0_i} [m]	2.5	2.5	2.5	2.5	2.5	2.5
γ_i	8.1652	9.9843	6.3392	9.9551	5.3818	-
ϱ_i	0.05	0.05	0.01	0.01	0.01	-
ϵ_i	0.01	10	0	0.3	0	-
λ_i	0.454	0.455	0.453	0.455	0.451	-
τ_{mad_i} (s)	0.037	0.03	0.048	0.030	0.057	-
τ_{miet_i} (s)	0.14	0.114	0.18	0.114	0.213	-
ε_i	0.01	0.01	0.01	0.01	0.01	-

It is assumed that the communication delay from vehicle 1 to vehicle 2 is equal to the maximum allowable delay τ_{mad_1}, and from vehicle 2 to vehicle 3 τ_{mad_2}, and the same principle holds for the remaining vehicles, as denoted in Table 5-1. All vehicles perform the computations at a frequency of 100 Hz. In the simulations, the vehicles in the platoon equipped with an event-triggered controller are compared to a vehicle platoon in which the vehicles are equipped with a time-triggered controller, in which communication is established at a frequency of 10 Hz.

The three scenario's are discussed separately in detail. For all three scenario's the $\mathcal{L}_2$-gain is evaluated by computing the $\mathcal{L}_2$-norm, as defined in Appendix A, of the controller $\chi_i, \quad i = 1...6$ over the simulation time, and evaluate if string-stability is actually violated. Furthermore, the $\mathcal{L}_2$-norm of the spacing error e_i is also computed for comparison purposes.

5-2 Simulation results for different driving scenario's

This section covers the simulation results for different typical driving maneuvers of the leader vehicle. The results depicted for each scenario for both compared platoons are: the controller χ_i, the transmitted wireless signal, the acceleration u_i, the intervehicle distance d_i, the vehicle velocity v_i, the spacing error e_i, and the inter-transmission times.

5-2-1 Normal highway driving

In normal highway driving the leader vehicle follows a velocity profile with gentle velocity increase and gentle velocity decrease. The profile used for the simulations is depicted in Figure 5-1.

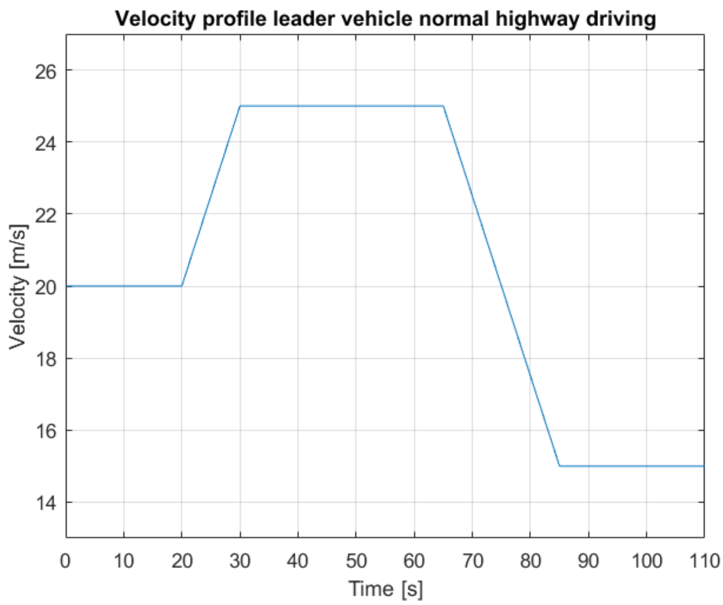

Figure 5-1: Velocity profile leader vehicle for normal highway driving

The simulation results for this scenario are depicted below.

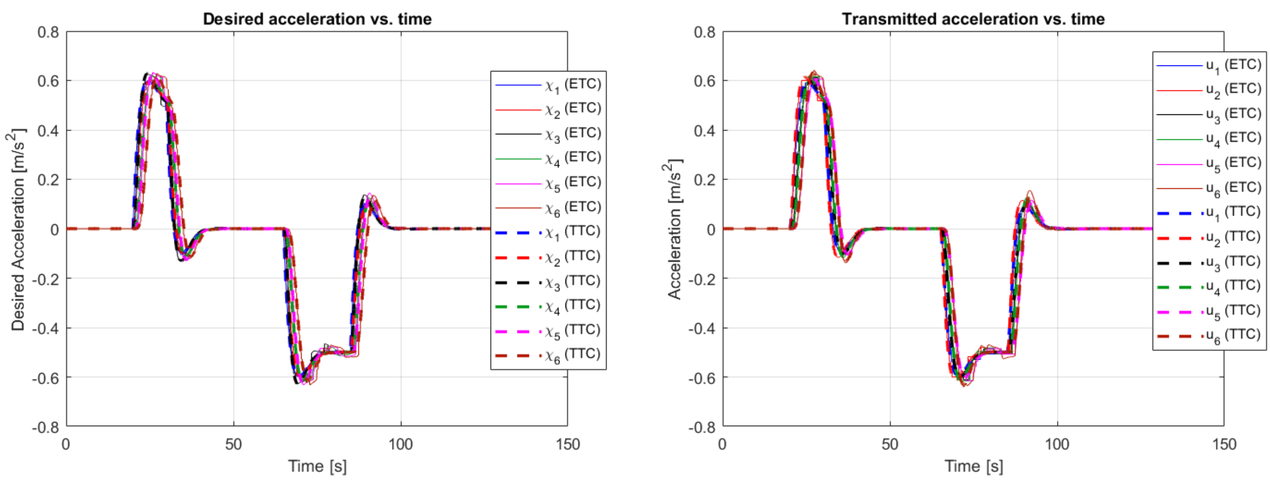

(a) The controller χ_i

(b) The transmitted acceleration u_i

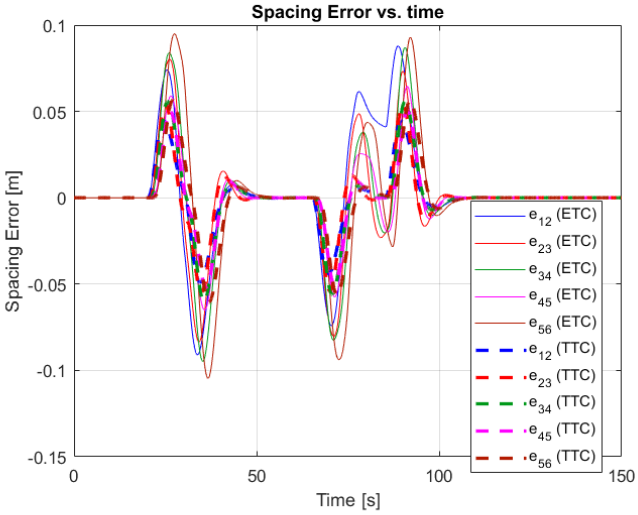

(c) The spacing error e_i

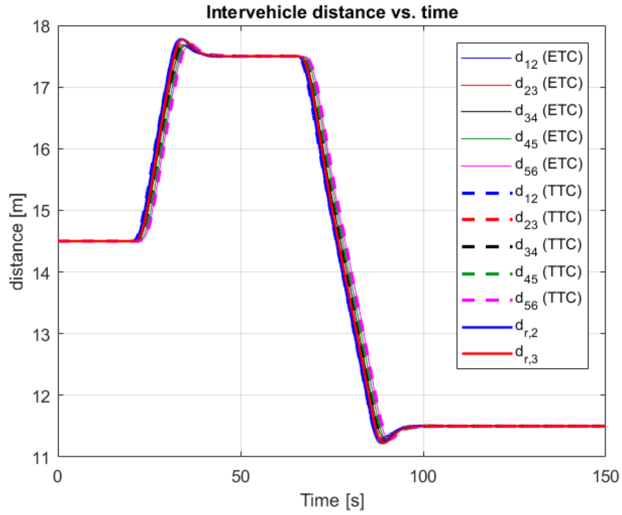

(d) The intervehicle distance d_i

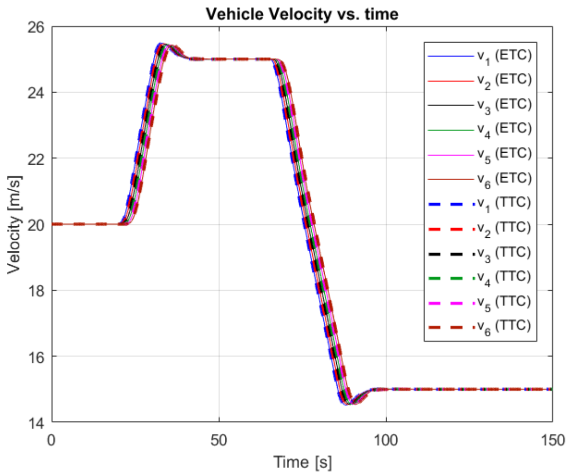

(e) The velocities v_i

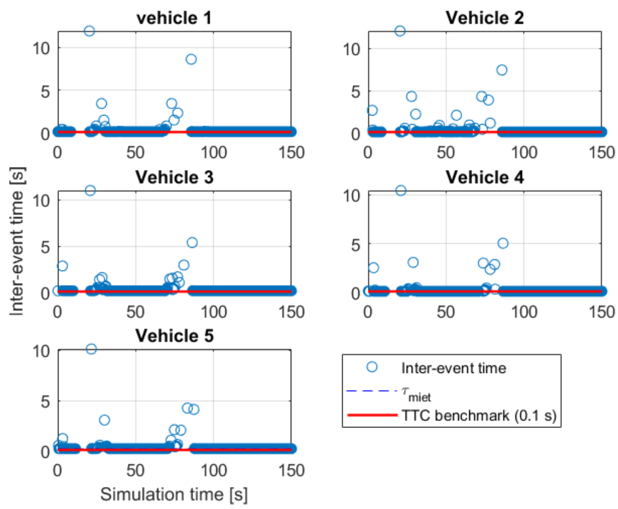

(f) The inter-transmission times

Figure 5-1: The simulation results for normal driving scenario

Discussion

In this section, we discuss the simulation results for the normal-driving scenario.

We start with Figure 5-1e, which depicts the velocity trajectory of each vehicle. It can be observed that the velocity profile that the leader vehicle must follow, is nicely followed by all vehicles in the platoon. It can be concluded that $v_i \to v_c \quad \forall i = 1, 2, 3$, with v_c the desired constant speed of the velocity trajectory of the leader. Furthermore, when comparing the two different platoons, the platoon equipped with periodic communication (TTC), and the platoon with aperiodic communication (ETC), it can be observed that the velocity trajectory for each vehicle is similar.

Next, we discuss the intervehicle distances from vehicle 2 to 1, and from vehicle 3 to 2, as depicted in Figure 5-1d. It can be observed that the intervehicle distance are equal for all vehicles, due to the same time headway h_i and the same velocity v_i. Next, it can be observed that the vehicles do not crash as the intervehicle distances are strictly positive.

Next, we discuss the spacing errors, which is depicted in Figure 5-1c. The spacing errors of the two different platoons (TTC and ETC) do not show similar responses. It can be observed that the ETC equipped vehicle platoon has more fluctuations in its spacing error response. However, it seems worse than it actually is, as the spacing error response for all vehicles is not greater than 0.1 m, with the maximum difference between the responses of the TTC and ETC equipped platoon 0.045 m. This implies similar closed-loop performance for the two platoons. Furthermore, it can be seen that the spacing error $e_i \to 0$ for constant velocity, and therefore, complying with Eq. (2-8).

Now, the responses of the controller, χ_i, and the communicated variable u_i, are observed, depicted in Figure 5-2a and Figure 5-2b. It can be observed that the closed-loop responses of χ_i and u_i are similar for the two different platoons, and the accelerations converge to zero, implying constant speed of each vehicle.

Observe Table 5-2, which displays the $\mathcal{L}_2$-norms of the controller χ_i, and spacing error e_i. Observe that string-stability is almost guaranteed as the $\mathcal{L}_2$-gain from χ_2 to χ_3 is indeed larger than 1. However, notice that when the $\mathcal{L}_2$-gain in terms of controller inputs is larger than 1, the $\mathcal{L}_2$-gain in terms of spacing errors is smaller than 1, e.g. for instance the $\mathcal{L}_2$-gain between vehicle 2 and 3 in terms of acceleration and spacing error. This suggests that the $\mathcal{L}_2$-gain stability in terms of acceleration does not simply carry over to $\mathcal{L}_2$-gain stability in terms of spacing error.

Table 5-2: $\mathcal{L}_2$-norm of χ_i, e_i, defined over time $[0, 150]$

	Vehicle 1	Vehicle 2	Vehicle 3	Vehicle 4	Vehicle 5	Vehicle 6
χ_i	28.81	28.72	29.36	28.83	29.01	28.69
e_i	-	3.80	3.29	3.61	2.46	4.09

Finally, the comparison in inter-transmission times is discussed, as depicted in Figure 5-1f. Firstly, the inter-transmission times are always lower-bounded by the minimum inter-event time τ_{miet}, which is a necessity. Next, it can be observed that the event-triggered controllers are decentralized, as the vehicles trigger at different instances. Finally, in Table 5-3, the number of inter transmissions, the average inter-transmission time, and the reduction in inter-transmission time compared to the TTC equipped platoon is outlined. Observe that the average inter-transmission time for both vehicles is already larger than its TTC counterpart. Next, it can be observed that a reduction of at least 39% is achieved when applying Event-Triggered Control for the communication, with the observation that the closed-loop performance is similar. This shows the advantage of event-triggered control over periodic control.

Table 5-3: Comparison of inter-transmission times between TTC and ETC for the vehicle platoons

	Inter-transmissions (#)	Average inter-transmission time (s)	Reduced number of events (%)
TTC	1500	0.1	-
Vehicle 1	706	0.2023	52.9
Vehicle 2	770	0.1848	48.7
Vehicle 3	615	0.2339	59
Vehicle 4	910	0.1548	39.3
Vehicle 5	520	0.2785	65.3

Remark 1. *Observe from Figure 5-1f that vehicles 1 and 2 are still transmitting to their respective successor vehicle when driving with constant speed, for instance after 100 seconds. This is unnecessary and suggests to add another condition to the current event-triggering mechanism. By adding the condition that communication can only be established for nonzero acceleration will eliminate communication after 100 seconds for instance. This reduces the communication from the current 39% to at least 50% while maintaining similar closed loop performance.*

5-2-2 Stop-And-Go

For a stop-and-go scenario we simulate driving in e.g. heavy traffic, in which the leader vehicle brake from an initial velocity to a full stop, starts accelerating again to a final speed, and then again brakes to a full stop. Its velocity profile is depicted in Figure 5-2.

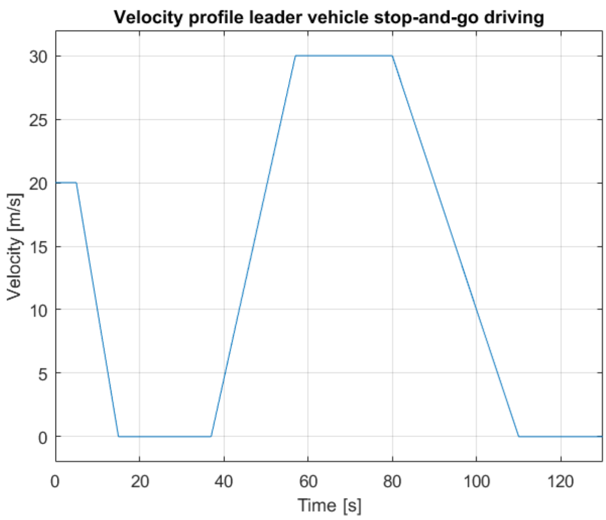

Figure 5-2: Velocity profile leader vehicle for stop-and-go scenario

The simulation results for this scenario are depicted below.

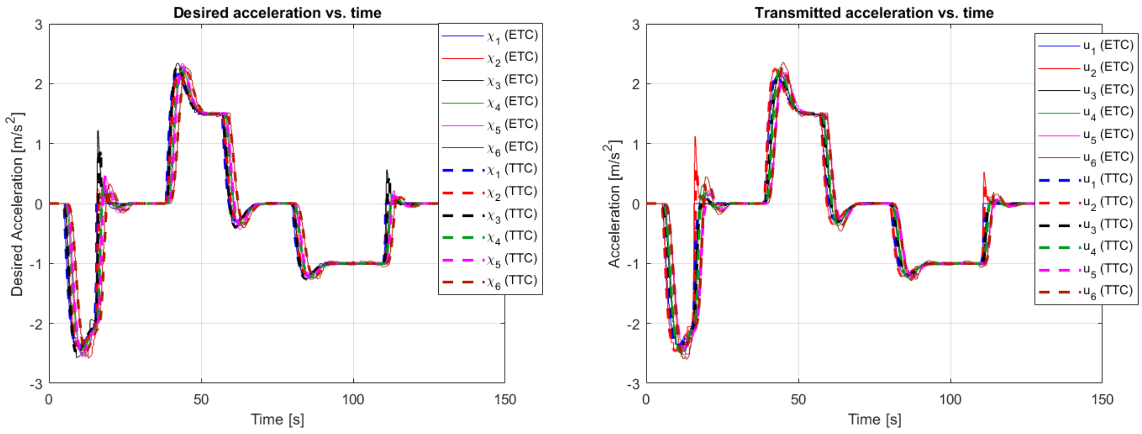

(a) The controller χ_i **(b)** The transmitted acceleration u_i

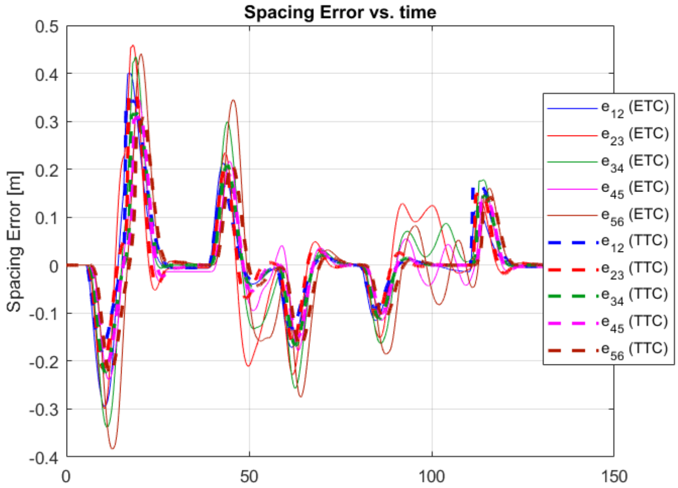

(c) The spacing error e_i

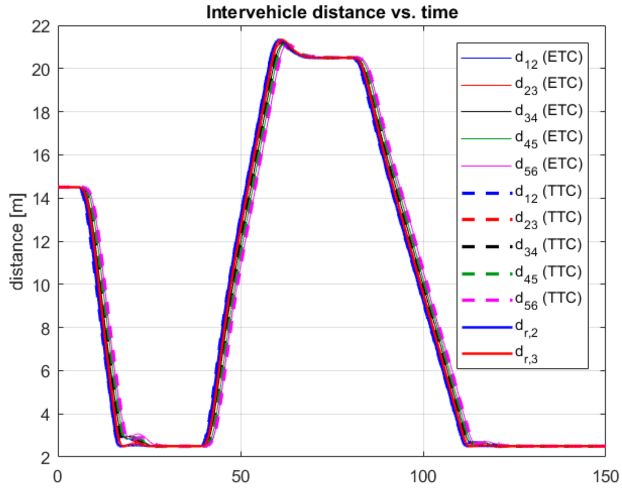

(d) The intervehicle distance d_i

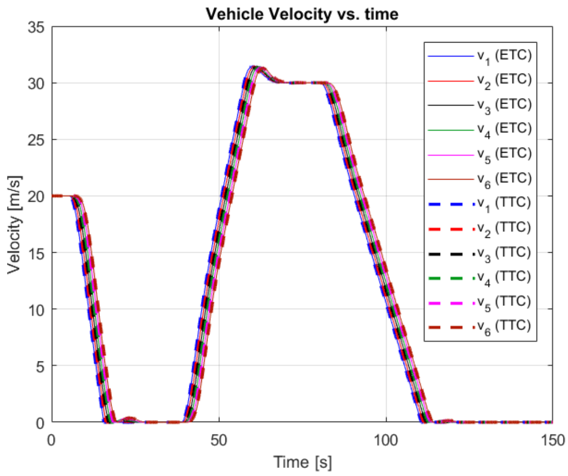

(e) The velocities v_i

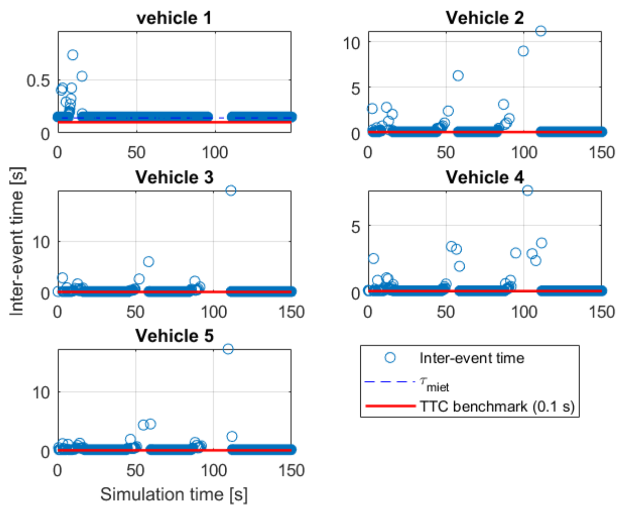

(f) The inter-transmission times

Figure 5-2: The simulation results for stop-and-go scenario

Discussion

In this section, we discuss the results for the stop-and-go scenario. It will not be discussed in detail, as the discussion follows along the same lines as the discussion about the normal driving scenario. It can be observed that all vehicles follow the velocity trajectory, that all vehicles have a strictly positive intervehicle distance, implying that no crashed occur. Furthermore, the spacing error converges to zero when the leader drives with constant speed, such that vehicle internal stability is preserved. However, it can also be observed that just as for the normal driving scenario, this scenario does not preserve string stability.

Observe from Table 5-4 that the string-stability is not guaranteed in terms of χ_i and spacing errors.

Finally, from Table 5-5 and Figure 5-2f it can be observed that the event-triggered controller reduces the communication significantly, while maintaining similar closed-loop performance compared to periodic communication.

Table 5-4: $\mathcal{L}_2$-norm of χ_i, e_i, defined over time $[0, 150]$

	Vehicle 1	Vehicle 2	Vehicle 3	Vehicle 4	Vehicle 5	Vehicle 6
χ_i	113.75	112.73	116.03	112.76	113.54	112.0
e_i	-	11.68	13.84	14.21	10.20	15.79

Table 5-5: Comparison of inter-transmission times between TTC and ETC for the vehicle platoons

	Inter-transmissions (#)	Average inter-transmission time (s)	Reduced number of events (%)
TTC	1500	0.1	-
Vehicle 1	794	0.1787	47
Vehicle 2	765	0.1860	49
Vehicle 3	558	0.2587	62.8
Vehicle 4	851	0.1662	43.3
Vehicle 5	467	0.3107	68.9

5-2-3 Emergency braking scenario

In this scenario the leader vehicle brakes heavily from an initial speed to full-stop, i.e. emergency braking. The goal of this scenario is to evaluate that vehicles do not crash into each other. The velocity profile for the leader vehicle for this maneuver is depicted in Figure 5-3.

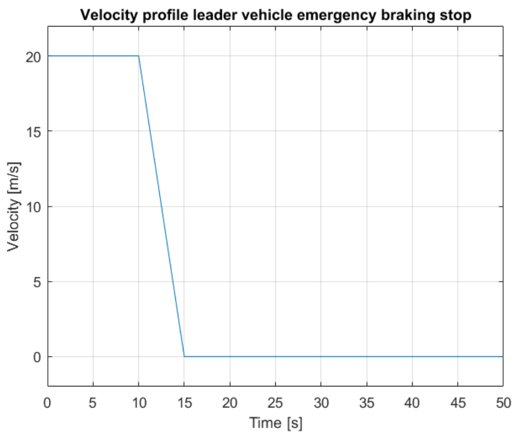

Figure 5-3: Velocity profile leader vehicle for emergency braking scenario

The simulation results for this scenario are depicted below.

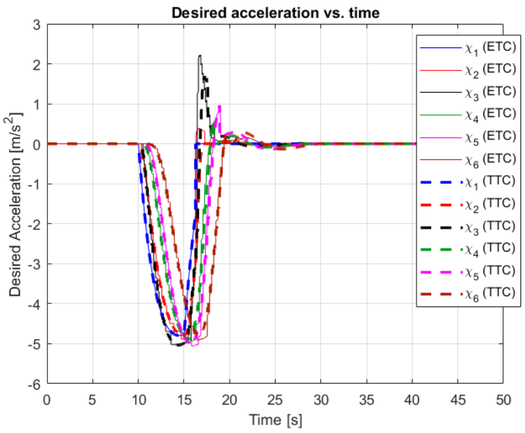

(a) The controller χ_i

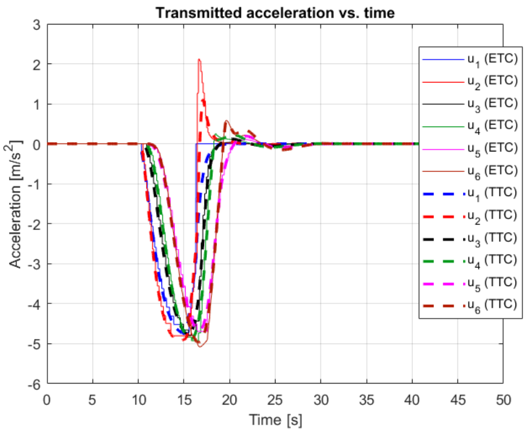

(b) The transmitted acceleration u_i

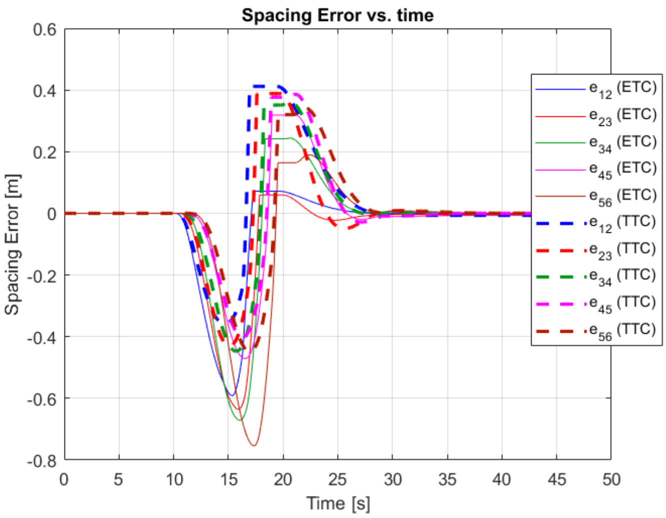

(c) The spacing error e_i

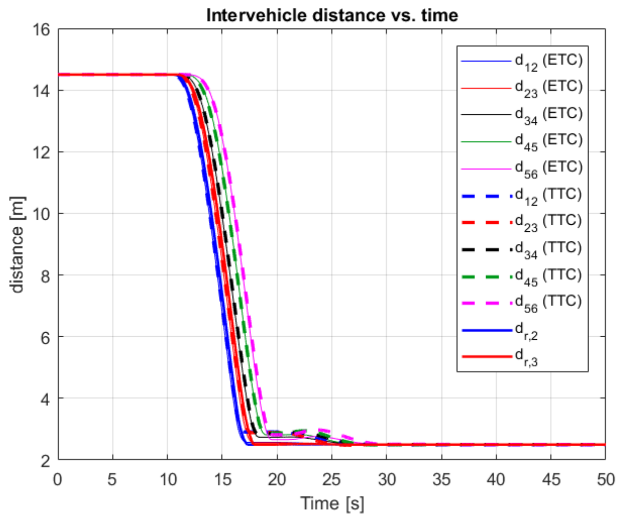

(d) The intervehicle distance d_i

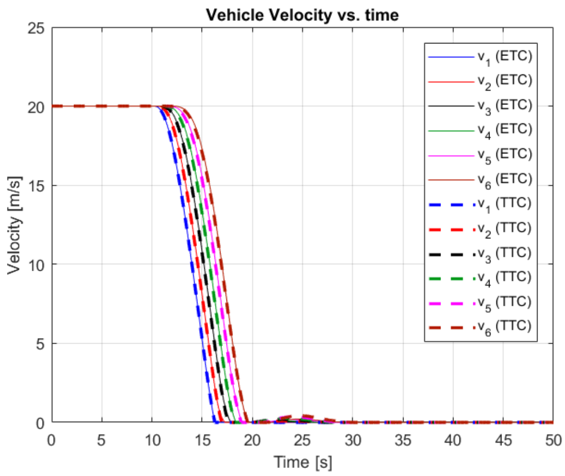

(e) The velocities v_i

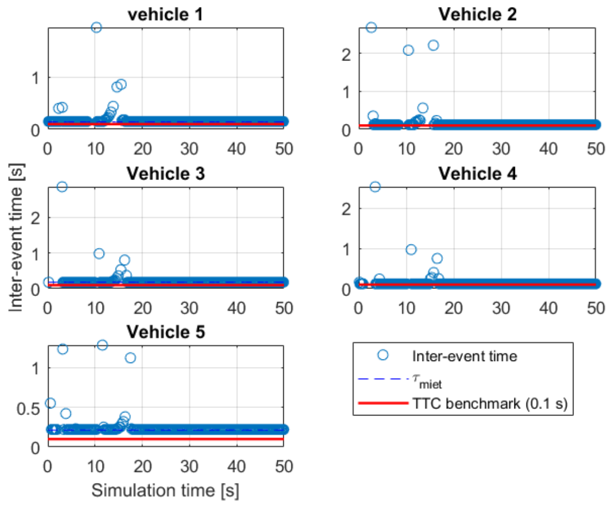

(f) The inter-transmission times

Figure 5-3: The simulation results for emergency braking

Discussion

In this section, a brief discussion is given about the simulation results for the emergency braking scenario. It is short and not in full detail, as the explanation is along the same lines as the discussion given for the normal driving scenario.

Firstly, it can be observed that the velocity of all vehicles converges to zero, while maintaining strictly positive inter-vehicle distance, and therefore, preventing a crash from happening. Next, the spacing error does converge to zero all vehicles.

Observe from Table 5-6 that string-stability is violated for this maneuver for the vehicle platoon.

Finally, it can be observed that similar closed-loop performance is achieved, while reducing communication significantly, showing the advantage of event-triggered control.

Table 5-6: $\mathcal{L}_2$-norm of χ_i, e_i, defined over time $[0, 50]$

	Vehicle 1	Vehicle 2	Vehicle 3	Vehicle 4	Vehicle 5	Vehicle 6
χ_i	93.93	91.48	101.1	91.94	94.23	89.72
e_i	-	10.29	11.18	12.78	10.33	13.69

Table 5-7: Comparison of inter-transmission times between TTC and ETC for the vehicle platoons

	Inter-transmissions (#)	Average inter-transmission time (s)	Reduced number of events (%)
TTC	500	0.1	-
Vehicle 1	283	0.1663	43.4
Vehicle 2	323	0.1447	35.4
Vehicle 3	236	0.2015	52.8
Vehicle 4	348	0.1336	30.4
Vehicle 5	200	0.2398	60

Chapter 6

Conclusion

Automated driving is a promising solution to increase traffic flow, road capacity, driving safety, and driving comfort. Vehicles are forming platoons, in which they follow one another with short intervehicle distances. Furthermore, shockwave effects can potentially be eliminated, which means string-stable behavior can be achieved. Current technology on the market as Adaptive Cruise Control (ACC) is not able to guarantee string-stable behavior. An extension to ACC, Cooperative Adaptive Cruise Control (CACC), is a promising solution for this, which lets vehicles cooperate by using communication.

Using Event-Triggered Control, continuous-time controllers are made resource-aware by determining when to transmit a new measurement to other vehicles. Furthermore, resources are used efficiently by transmitting only when it is necessary, reducing potential reliability issues while maintaining desired closed-loop performance.

In this thesis, Event-Triggered Controllers are designed for CACC, which is resource-aware and decentralized, to guarantee vehicle following for heterogeneous vehicle platoons. Furthermore, a weaker form of string stability is guaranteed for sufficient conditions, and in the presence of communication delays. Finally, a strictly positive minimum inter-event time is guaranteed.

Simulations are carried out to backup the mathematical results, and a comparison is made with the time-triggered paradigm, and it is shown that the event-triggering mechanism reduces the communication significantly, while maintaining similar closed-loop performance.

Future work

There are open problems that still need to be solved. Firstly, the guarantee of string-stable behavior of the vehicle platoon in presence of aperiodic communication and communication delays for a vehicle platoon. A possible solution for this is by using a different communication topology, such as the bidirectional topology, or the two-vehicle look-ahead, which gives additional information for tighter control. The challenge lies in formally guaranteeing this, and develop an algorithm, which is computationally tractable. Other open problems are the presence of constraints, such as actuator constraints and safety constraints, and guarantee of desired closed-loop performance in presence of measurement noise.

Appendix A

Preliminary mathematical notation

The following notation is going to be used in the thesis.

$\mathbb{N}$ denotes the set of all non-negative integers. $\mathbb{R}$ denotes the set of all real numbers, and $\mathbb{R}_{\leq 0}$ the set of all non-negative real numbers. For a matrix $P \in \mathbb{R}^{n \times n}$, $P \succeq 0$, P is symmetrix and positive semi-definite, such that $x^T P x \geq 0 \quad \forall x \neq 0$. Also, $P \preceq 0$ denotes a symmetrix matrix P that is negative semi-definite, such that $x^T P x \leq 0 \quad \forall x \neq 0$. A function $\beta(\cdot)$ is said to be of class $\mathcal{K}_\infty$-functions, if it is continuous, strictly increasing, $\beta(0) = 0$, and $\lim_{t \to \infty} \beta(r) = \infty$.

The $\mathcal{L}_2$-gain of a input-output system is used in the design of the controllers. Therefore, its definition is given below.

Definition 1. *The $\mathcal{L}_2$-norm of a function $u(\cdot)$, defined on $[0, \infty)$, is defined as*

$$||u||_{\mathcal{L}_2} = \sqrt{\int_0^\infty u^T(t) u(t) dt} \tag{A-1}$$

If $||u||_{\mathcal{L}_2} < \infty$, then $u \in \mathcal{L}_2$.

Definition 2. *A system with input u and output y has a finite $\mathcal{L}_2$-gain if there exist a nonnegative constant γ, and a class $\mathcal{K}$-function β, defined on $[0, \infty)$ such that [22]*

$$||y||_{\mathcal{L}_2} \leq \gamma ||u||_{\mathcal{L}_2} + \beta(||x(0)||) \tag{A-2}$$

which should hold for the initial condition $x(0)$, for any $u(\cdot)$ and any solution.

Appendix B

Design of Continuous Time CACC

B-1 Introduction

This section covers the design of a vehicle platooning controller in continuous-time. The design is an extension of [7] to heterogeneous vehicles, and serves as a recommendation on how to design linear continuous-time controllers for CACC. It gives a derivation of the plant dynamics used in the design of the controller, the controller structure, and guaranteed internal stability. This section refers to the plant dynamics given in Chapter 2, and Section 3-2.

B-2 The control law

The plant dynamics considered are adopted from [7].

$$\begin{pmatrix} \dot{e}_i(t) \\ \dot{v}_i(t) \\ \dot{a}_i(t) \end{pmatrix} = \begin{pmatrix} v_{i-1}(t) - v_i(t) - h_i a_i(t) \\ a_i(t) \\ -\frac{1}{\tau_{d_i}} a_i(t) + \frac{1}{\tau_{d_i}} u_i(t) \end{pmatrix} \quad i = 1...N \tag{B-1}$$

with e_i the spacing error as defined in Eq. (2-3), v_i the vehicle speed, a_i the vehicle's acceleration, and u_i the input. τ_{d_i} is a time constant representing the vehicle driveline dynamics.

To start with the control design, the following control law defining the error states, is used, which is formulated for a general vehicle platoon:

$$\begin{pmatrix} e_{1,i} \\ e_{2,i} \\ e_{3,i} \end{pmatrix} = \begin{pmatrix} e_i \\ \dot{e}_i \\ \ddot{e}_i \end{pmatrix}, \quad i = 1...N \tag{B-2}$$

with $\dot{e}_{1,i} = e_{2,i}$, and $\dot{e}_{2,i} = e_{3,i}$. The derivative of $e_{3,i}$ is given below:

$$\dot{e}_{3,i} = e_{3,i}^{(3)} = \dot{a}_{i-1} - \dot{a}_i - h_i\ddot{a}_i \tag{B-3}$$

$$\overset{(B-1)}{=} \frac{1}{\tau_{d_{i-1}}}(-a_{i-1} + u_{i-1}) - \frac{1}{\tau_{d_i}}(-a_i + u_i) - \frac{h_i}{\tau_{d_i}}(-\dot{a}_i + \dot{u}_i) \tag{B-4}$$

$$= \frac{1}{\tau_{d_{i-1}}}(-a_{i-1} + u_{i-1}) - \frac{1}{\tau_{d_i}}(-a_i + u_i) - \frac{h_i}{\tau_{d_i}}\left(\dot{u}_i - \frac{1}{\tau_i}(-a_i + u_i)\right) \tag{B-5}$$

Next, we solve a set of equations to get a differential equation with both $e_{3,i}$ and $\dot{e}_{3,i}$. This is done by using the following equations.

$$e_{3,i} = \ddot{e}_i = a_{i-1} - a_i - h_i\dot{a}_i = a_{i-1} - a_i - \frac{h_i}{\tau_{d_i}}(-a_i + u_i) \tag{B-6}$$

$$\dot{e}_{3,i} = \frac{1}{\tau_{d_{i-1}}}(-a_{i-1} + u_{i-1}) - \frac{1}{\tau_{d_i}}(-a_i + u_i) - \frac{h_i}{\tau_{d_i}}\left(\dot{u}_i - \frac{1}{\tau_{d_i}}(-a_i + u_i)\right) \tag{B-7}$$

$$\begin{pmatrix} e_{3,i} \\ \dot{e}_{3,i} \end{pmatrix} = \underbrace{\begin{pmatrix} 1 & \frac{h_i}{\tau_{d_i}} - 1 \\ -\frac{1}{\tau_{d_{i-1}}} & \frac{1}{\tau_{d_i}} - \frac{h_i}{\tau_{d_i}^2} \end{pmatrix}}_{V_1} \begin{pmatrix} a_{i-1} \\ a_i \end{pmatrix} + \underbrace{\begin{pmatrix} -\frac{h_i}{\tau_{d_i}} & 0 & 0 \\ \frac{h_i}{\tau_{d_i}^2} - \frac{1}{\tau_{d_i}} & -\frac{h_i}{\tau_{d_i}} & \frac{1}{\tau_{d_{i-1}}} \end{pmatrix}}_{V_2} \begin{pmatrix} u_i \\ \dot{u}_i \\ u_{i-1} \end{pmatrix} \tag{B-8}$$

Next, Eq. (B-8) is solved for a_{i-1}, a_i. This requires V_1 to be invertible, which holds $\forall\, \tau_{d_{i-1}} \setminus \{\tau_{d_i}\} \wedge \{h_i, \tau_{d_i}\} \setminus \{1, 1\}$.

Finally, inserting the solution of Eq. (B-8), a_{i-1} into Eq. (B-6), and then solving for $\dot{e}_{3,i}$ gives the following equation.

$$\dot{e}_{3,i} = -\frac{1}{\tau_{d_{i-1}}}e_{3,i} + \left(-\frac{1}{\tau_{d_{i-1}}} + \frac{1}{\tau_{d_i}} - \frac{h_i}{\tau_{d_i}^2} + \frac{h_i}{\tau_{d_{i-1}}\tau_{d_i}}\right)a_i + \left(-\frac{1}{\tau_{d_i}} + \frac{h_i}{\tau_{d_i}^2} - \frac{h_i}{\tau_{d_{i-1}}\tau_{d_i}}\right)u_i - \frac{h_i}{\tau_{d_i}}\dot{u}_i + \frac{1}{\tau_{d_{i-1}}}u_{i-1} \tag{B-9}$$

By defining the input χ_i as

$$\chi_i = \left(1 - \frac{\tau_{d_{i-1}}}{\tau_{d_i}} + \frac{h_i\tau_{d_{i-1}}}{\tau_{d_i}^2} - \frac{h_i}{\tau_{d_i}}\right)a_i + \left(\frac{\tau_{d_{i-1}}}{\tau_{d_i}} - \frac{h_i\tau_{d_{i-1}}}{\tau_{d_i}^2} + \frac{h_i}{\tau_{d_i}}\right)u_i + \frac{h_i\tau_{d_{i-1}}}{\tau_{d_i}}\dot{u}_i \tag{B-10}$$

Eq. (B-9) becomes

$$\dot{e}_{3,i} = -\frac{1}{\tau_{d_{i-1}}}e_{3,i} - \frac{1}{\tau_{d_{i-1}}}\chi_i + \frac{1}{\tau_{d_{i-1}}}u_{i-1} \tag{B-11}$$

It becomes clear from Eq. (B-11) that χ_i must be designed to stabilize the error dynamics and compensate for u_{i-1} in order to get exact vehicle following. Hence, χ_i is chosen as follows.

$$\chi_i = \underbrace{\begin{pmatrix} k_{p_i} & k_{d_i} & k_{dd_i} \end{pmatrix} \begin{pmatrix} e_{1,i} \\ e_{2,i} \\ e_{3,i} \end{pmatrix}}_{ACC} + \underbrace{u_{i-1}}_{CACC}, \quad i = 1...N \tag{B-12}$$

with k_{p_i}, k_{d_i}, and k_{dd_i} gains on the errors $e_{1,i}$, $e_{2,i}$, and $e_{3,i}$ respectively, and u_{i-1} a feedforward term acquired through wireless communication from the predecessor vehicle. The feedback controller is usually referred to as the ACC part of the controller, and the feedforward term is referred to as the CACC part of the controller. [3, 19]

Substituting Eq. (B-10) into Eq. (B-12), we get the following expression for $\dot{u}_i$, which is defined as the controller dynamics.

$$\dot{u}_i = \frac{\tau_{d_i}}{h_i \tau_{d_{i-1}}} \left(\begin{pmatrix} k_{p_i} & k_{d_i} & k_{dd_i} \end{pmatrix} \begin{pmatrix} e_{1,i} \\ e_{2,i} \\ e_{3,i} \end{pmatrix} + u_{i-1} \right) + \frac{\tau_{d_i}}{h_i \tau_{d_{i-1}}} \left(-1 + \frac{\tau_{d_{i-1}}}{\tau_{d_i}} - \frac{h_i \tau_{d_{i-1}}}{\tau_{d_i}^2} + \frac{h_i}{\tau_{d_i}} \right) a_i - \frac{\tau_{d_i}}{h_i \tau_{d_{i-1}}} \left(\frac{\tau_{d_{i-1}}}{\tau_{d_i}} - \frac{h_i \tau_{d_{i-1}}}{\tau_{d_i}^2} + \frac{h_i}{\tau_{d_i}} \right) u_i \quad \text{(B-13)}$$

The error states in Eq. (B-2), the controller dynamics in Eq. (B-13), and the differential equation for a_i, given in Eq. (B-1) for completeness, are combined in one state-space equation, which is given below.

$$\begin{pmatrix} \dot{e}_{1,i} \\ \dot{e}_{2,i} \\ \dot{e}_{3,i} \\ \dot{u}_i \\ \dot{a}_i \end{pmatrix} = \underbrace{\left(\begin{array}{ccc|cc} 0 & 1 & 0 & 0 & 0 \\ 0 & 0 & 1 & 0 & 0 \\ -\frac{k_{p_i}}{\tau_{d_{i-1}}} & -\frac{k_{d_i}}{\tau_{d_{i-1}}} & -\frac{1+k_{dd_i}}{\tau_{d_{i-1}}} & 0 & 0 \\ \hline \frac{k_{p_i}\tau_{d_i}}{h_i\tau_{d_{i-1}}} & \frac{k_{d_i}\tau_{d_i}}{h_i\tau_{d_{i-1}}} & \frac{k_{dd_i}\tau_{d_i}}{h_i\tau_{d_{i-1}}} & \frac{\tau_{d_i}}{h_i\tau_{d_{i-1}}}\left(-\frac{\tau_{d_{i-1}}}{\tau_{d_i}} + \frac{h_i\tau_{d_{i-1}}}{\tau_{d_i}^2} - \frac{h_i}{\tau_{d_i}}\right) & \frac{\tau_{d_i}}{h_i\tau_{d_{i-1}}}\left(-1 + \frac{\tau_{d_{i-1}}}{\tau_{d_i}} - \frac{h_i\tau_{d_{i-1}}}{\tau_{d_i}^2} + \frac{h_i}{\tau_{d_i}}\right) \\ 0 & 0 & 0 & \frac{1}{\tau_{d_i}} & -\frac{1}{\tau_{d_i}} \end{array} \right)}_{Z_i} \begin{pmatrix} e_{1,i} \\ e_{2,i} \\ e_{3,i} \\ u_i \\ a_i \end{pmatrix} + \begin{pmatrix} 0 \\ 0 \\ 0 \\ \frac{\tau_{d_i}}{h_i\tau_{d_{i-1}}} \\ 0 \end{pmatrix} u_{i-1} \quad \text{(B-14)}$$

B-3 Guarantee of internal vehicle stability

The stability of Z_i is analyzed, for which a Lemma is formulated.

Lemma 2. *Consider Z_i as in Eq. (B-14). Then Z_i is asymptotically stable for any $h_i, \tau_{d_{i-1}}, \tau_{d_i}, k_{p_i}, k_{d_i} > 0, k_{dd_i} > -1$ iff $(1 + k_{dd_i})\, k_{d_i} > k_{p_i}\tau_{d_{i-1}}$ holds.*

Proof. Firstly, observe that Z_i is block-triangular, which means that the eigenvalues of Z_i are equal to the eigenvalues of the upper-left and the lower-right matrix. Therefore, we analyze for which conditions these two matrices are asymptotically stable.

We start with the upper-left matrix. It can easily be seen that the characteristic polynomial is equal to

$$s^3 + \underbrace{\frac{1 + k_{dd_i}}{\tau_{d_{i-1}}}}_{a_2} s^2 + \underbrace{\frac{k_{d_i}}{\tau_{d_{i-1}}}}_{a_1} s + \underbrace{\frac{k_{p_i}}{\tau_{d_{i-1}}}}_{a_0} \quad \text{(B-15)}$$

Next, we apply the Routh-Hurwitz stability criterion. for a third order polynomial $a_3 s^3 + a_2 s^2 + a_1 s + a_0$, the roots are negative iff $a_0, a_2 > 0, a_2 a_1 > a_0$. Applying this, we get the following inequality.

$$\left(\frac{1 + k_{dd_i}}{\tau_{d_{i-1}}}\right)\left(\frac{k_{d_i}}{\tau_{d_{i-1}}}\right) > \left(\frac{k_{p_i}}{\tau_{d_{i-1}}}\right) \tag{B-16}$$

Multiplying left and right-hand side with $\tau_{d_{i-1}}^2$, we get the inequality $(1 + k_{dd_i})\, k_{d_i} > k_{p_i}\tau_{d_{i-1}}$. Furthermore, $a_2, a_0 > 0$ holds for $k_{dd_i} > -1, k_{d_i}, k_{p_i} > 0, \tau_{d_{i-1}} > 0$.

Next, we consider the lower-right matrix, which is a 2x2 matrix. A 2x2 matrix is Hurwitz iff its trace is negative, and its determinant is positive. Applying this gives the following condition for the trace.

$$\frac{\tau_{d_i}}{h_i \tau_{d_{i-1}}}\left(-\frac{\tau_{d_{i-1}}}{\tau_{d_i}} + \frac{h_i \tau_{d_{i-1}}}{\tau_{d_i}^2} - \frac{h_i}{\tau_{d_i}}\right) - \frac{1}{\tau_{d_i}} < 0 \tag{B-17}$$

$$-\frac{1}{h_i} + \frac{1}{\tau_{d_i}} - \frac{1}{\tau_{d_{i-1}}} - \frac{1}{\tau_{d_i}} < 0 \tag{B-18}$$

$$-\frac{1}{h_i} - \frac{1}{\tau_{d_{i-1}}} < 0 \tag{B-19}$$

which holds for all $h_i, \tau_{d_{i-1}}, \tau_{d_i} > 0$.

Next, the determinant must be positive, which holds if

$$-\frac{\tau_{d_i}}{h_i \tau_{d_{i-1}}}\left(-\frac{\tau_{d_{i-1}}}{\tau_{d_i}} + \frac{h_i \tau_{d_{i-1}}}{\tau_{d_i}^2} - \frac{h_i}{\tau_{d_i}}\right)\frac{1}{\tau_{d_i}} - \frac{\tau_{d_i}}{h_i \tau_{d_{i-1}}}\left(-1 + \frac{\tau_{d_{i-1}}}{\tau_{d_i}} - \frac{h_i \tau_{d_{i-1}}}{\tau_{d_i}^2} + \frac{h_i}{\tau_{d_i}}\right)\frac{1}{\tau_{d_i}} > 0 \tag{B-20}$$

$$-\frac{\tau_{d_i}}{h_i \tau_{d_{i-1}}}\left(-\frac{\tau_{d_{i-1}}}{\tau_{d_i}} + \frac{h_i \tau_{d_{i-1}}}{\tau_{d_i}^2} - \frac{h_i}{\tau_{d_i}} - 1 + \frac{\tau_{d_{i-1}}}{\tau_{d_i}} - \frac{h_i \tau_{d_{i-1}}}{\tau_{d_i}^2} + \frac{h_i}{\tau_{d_i}}\right)\frac{1}{\tau_{d_i}} > 0 \tag{B-21}$$

$$1 > 0 \tag{B-22}$$

which always holds.

To conclude the proof, Z_i is asymptotically stable iff $h_i, \tau_{d_{i-1}}, \tau_{d_i}, k_{p_i}, k_{d_i} > 0, k_{dd_i} > -1$, and $(1 + k_{dd_i})\, k_{d_i} > k_{p_i}\tau_{d_{i-1}}$. □

Translating the result of Lemma 2 to the physical system, it means that the vehicle is internally stable.

Remark 2. *Note that when a homogeneous vehicle platoon is considered, i.e.* $\tau_{d_{i-1}} = \tau_{d_i} = \tau_d$, *the original result of [7] is obtained.*

It must be noted that according to Lemma 2, for the design of the feedback controllers gains k_{p_i} and k_{d_i}, the time constant $\tau_{d_{i-1}}$ of the predecessor vehicle is necessary. It is assumed this constant is known to vehicle i.

The third-order model defined in Eq. (B-1) is extended with the controller dynamics given in Eq. (B-13), such that the following fourth-order model is used throughout the thesis.

$$\begin{pmatrix} \dot{e}_i(t) \\ \dot{v}_i(t) \\ \dot{a}_i(t) \\ \dot{u}_i(t) \end{pmatrix} = \begin{pmatrix} v_{i-1}(t) - v_i(t) - h_i a_i(t) \\ a_i(t) \\ -\frac{1}{\tau_{d_i}} a_i(t) + \frac{1}{\tau_{d_i}} u_i(t) \\ \hline O_i \left(Q_i a_i(t) - R_i u_i(t) + \chi_i(t) \right) \end{pmatrix}, \quad i = 1...N \tag{B-23}$$

with O_i, Q_i, R_i as in Eq. (2-5)-(2-7), and with the controller χ_i given as

$$\chi_i(t) = k_{p_i} e_i(t) + k_{d_i} \dot{e}_i(t) + k_{dd_i} \ddot{e}_i(t) + u_{i-1}(t) \tag{B-24}$$

$$O_i = \frac{\tau_{d_i}}{h_i \tau_{d_{i-1}}} \tag{B-25}$$

$$Q_i = -1 + \frac{\tau_{d_{i-1}}}{\tau_{d_i}} - \frac{h_i \tau_{d_{i-1}}}{\tau_{d_i^2}} + \frac{h_i}{\tau_{d_i}} \tag{B-26}$$

$$R_i = \frac{\tau_{d_{i-1}}}{\tau_{d_i}} - \frac{h_i \tau_{d_{i-1}}}{\tau_{d_i}^2} + \frac{h_i}{\tau_{d_i}} \tag{B-27}$$

Appendix C

Proof of Theorem 1

To proof finite $\mathcal{L}_2$-gain from χ_i to χ_{i+1}, we aim to find positive semi-definite storage function S_i of the state for the pair of adjacent vehicles defined by Eq. (3-21)-Eq. (3-22) that satisfies [26]

$$\dot{S}_i \leq (1+\epsilon_i)|\chi_i|^2 - |\chi_{i+1}|^2, \quad i = 0...N-1 \tag{C-1}$$

in between events, and

$$S_i(\xi_i^+) - S_i(\xi_i) \leq 0 \tag{C-2}$$

during jumps.

Consider the following positive semi-definite candidate storage function U_i. It will be shown that $S_i = \dfrac{U_i}{\mu_i}$ satisfies Eq. (C-1) and Eq. (C-2), with $\mu_i \in \mathbb{R}_{>0}$ one of the solutions to the Linear Matrix Inequality, with the matrix given in Eq. (3-30).

$$U_i = V(\tilde{x}_i) + \eta_i + \gamma_{l_i}\phi_{l_i}(\tau_i)W_i^2(e_{u_i}) \tag{C-3}$$

with $V(\tilde{x}_i) = \tilde{x}_i^T P_i \tilde{x}_i$, and $P_i = P_i^T \succeq 0$ a positive semi-definite matrix, for which $M_i \preceq 0$ holds, with M_i defined in Eq. (3-30), and η_i the triggering variable as in Eq. (3-7), and $\phi_{l_i}(\tau_i)$ defined in Eq. (3-9).

W_i is a positive semi-definite function of the network-induced error e_{u_i}.

$$W_i(e_{u_i}) := |e_{u_i}| \tag{C-4}$$

Before we look at the evolution of U_i, we look at the evolution of V_i, η_i, $W_i(e_{u_i})$.

The evolution of V_i is treated first. Its derivative is equal to the following expression, using Eq. (3-21) for $\dot{\tilde{x}}_i$.

$$\dot{V}_i = \dot{\tilde{x}}_i^T P_i \tilde{x}_i + \tilde{x}_i^T P_i \dot{\tilde{x}}_i = (A_{11_i}\tilde{x}_i + A_{12_i}e_{u_i} + A_{13_i}\chi_i)^T P_i \tilde{x}_i + \tilde{x}_i^T P_i (A_{11_i}\tilde{x}_i + A_{12_i}e_{u_i} + A_{13_i}\chi_i)$$

Next, we use the condition that $M_i \preceq 0$, with M_i given in Eq. (3-30). Substituting χ_{i+1} from Eq. (3-22), with C_{z_i} and D_{z_i} as in Eq. (3-28) and Eq. (3-29) respectively, and using Eq. (3-26) for u_i and Eq. (3-27) for a_i, we get the following inequality for $\dot{V}_i$.

$$\begin{aligned}\dot{V}_i \leq & -\varrho_i \tilde{x}_i^T C_1^T C_1 \tilde{x}_i - O_i^2 \Big((-\chi_i + (R_i C_1 - Q_i C_2)\,\tilde{x}_i)^T (-\chi_i + (R_i C_1 - Q_i C_2)\,\tilde{x}_i) \Big) + \\ & \mu_i \Big((1+\epsilon_i)\chi_i^T \chi_i - (C_{z_i}\tilde{x}_i + D_{z_i} e_{u_i})^T (C_{z_i}\tilde{x}_i + D_{z_i} e_{u_i}) \Big) + \gamma_{l_i}^2 e_{u_i}^T e_{u_i} \qquad \text{(C-5)} \\ \leq & -\varrho_i u_i^2 - O_i^2(-\chi_i - Q_i a_i + R_i u_i)^2 + \mu_i((1+\epsilon_i)|\chi_i|^2 - |\chi_{i+1}|^2) + \gamma_{l_i}^2 e_{u_i}^2 \qquad \text{(C-6)}\end{aligned}$$

Finally, the evolution of W_i in between events is given below.

$$\begin{aligned}\dot{W}_i =& \frac{d}{dt}|e_{u_i}| \\ =& sgn(e_{u_i})\dot{e}_{u_i} \quad \Big(\textit{From this, } \dot{W}_i \leq |\dot{e}_{u_i}|, \textit{ therefore} \Big) \\ \dot{W}_i \leq & |\dot{e}_{u_i}| = O_i |R_i u_i - \chi_i - Q_i a_i| \qquad \text{(C-7)}\end{aligned}$$

As $\dot{V}_i$, $\dot{\eta}_i$, $\dot{\phi}_{l_i}(\tau_i)$, and $\dot{W}_i$ are defined, the evolution of U_i is now considered.

$$\begin{aligned}\dot{U}_i \leq & \dot{V}_i + 2\gamma_{l_i}\phi_{l_i} W_i \dot{W}_i + \gamma_{l_i}\dot{\phi}_{l_i} W_i^2 + \dot{\eta}_i \qquad \text{(C-8)} \\ & \textit{(Fill in Eq. (C-6) for } \dot{V}_i\textit{, Eq. (3-7) for } \dot{\eta}_i\textit{, Eq. (C-7) for } \dot{W}_i\textit{, and Eq. (3-9) for } \dot{\phi}\textit{)} \\ \leq & -\varrho_i u_i^2 - O_i^2 |R_i u_i - \chi_i - Q_i a_i|^2 + \mu_i((1+\epsilon_i)|\chi_i|^2 - |\chi_{i+1}|^2) + \gamma_{l_i}^2 e_{u_i}^2 + \\ & 2\gamma_{l_i}\phi_{l_i} W_i \left(O_i |R_i u_i - \chi_i - Q_i a_i|\right) - (1-\omega(\tau_i))\gamma_{l_i}^2(\phi_{l_i}^2 + 1) W_i^2 + \\ & \varrho_i u_i^2 + \omega(\tau_i) \left((1-\varepsilon_i)\, O_i^2 |R_i u_i - \chi_i - Q_i a_i|^2 - \gamma_{l_i}^2 (1 + \frac{1}{\varepsilon_i}\phi_{l_i}^2) e_{u_i}^2 \right) \qquad \text{(C-9)} \\ & \textit{(Using Eq. (C-4), we get } W_i = |e_{u_i}|\textit{)} \\ \leq & -\varrho_i u_i^2 - O_i^2 |R_i u_i - \chi_i - Q_i a_i|^2 + \mu_i((1+\epsilon_i)|\chi_i|^2 - |\chi_{i+1}|^2) + \gamma_{l_i}^2 W_i^2 + \\ & 2\gamma_{l_i}\phi_{l_i} W_i \left(O_i |R_i u_i - \chi_i - Q_i a_i|\right) - (1-\omega(\tau_i))\gamma_{l_i}^2(\phi_{l_i}^2 + 1) W_i^2 + \\ & \varrho_i u_i^2 + \omega(\tau_i) \left((1-\varepsilon_i)\, O_i^2 |R_i u_i - \chi_i - Q_i a_i|^2 - \gamma_{l_i}^2 (1 + \frac{1}{\varepsilon_i}\phi_{l_i}^2) W_i^2 \right) \qquad \text{(C-10)} \\ & \textit{(Simplifying the right-hand side of the inequality)} \\ \leq & -O_i^2 |R_i u_i - \chi_i - Q_i a_i|^2 + \mu_i((1+\epsilon_i)|\chi_i|^2 - |\chi_{i+1}|^2) + 2\gamma_{l_i}\phi_{l_i} W_i \left(O_i |R_i u_i - \chi_i - Q_i a_i|\right) - \\ & \gamma_{l_i}^2 \phi_{l_i}^2 W_i^2 + \omega(\tau_i) \left((1-\varepsilon_i)\, O_i^2 |R_i u_i - \chi_i - Q_i a_i|^2 + \gamma_{l_i}^2 \left(1 - \frac{1}{\varepsilon_i}\right) \phi_{l_i}^2 W_i^2 \right) \\ & \textit{(Using the completion-of-squares, we can write the above inequality in the following form)} \\ \leq & (\omega(\tau_i) - 1)\left(O_i |R_i u_i - \chi_i - Q_i a_i| - \gamma_{l_i}\phi_{l_i} W_i\right)^2 - \\ & \omega(\tau_i) \left(\varepsilon_i O_i^2 |R_i u_i - \chi_i - Q_i a_i|^2 + \gamma_{l_i}^2 \frac{1}{\varepsilon_i} \phi_{l_i}^2 W_i^2 + 2\gamma_{l_i}\phi_{l_i} W_i O_i |R_i u_i - \chi_i - Q_i a_i| \right) \\ & + \mu_i \left((1+\epsilon_i)|\chi_i|^2 - |\chi_{i+1}|^2 \right) \\ \leq & (\omega(\tau_i) - 1)\left(O_i |R_i u_i - \chi_i - Q_i a_i| - \gamma_{l_i}\phi_{l_i} W_i\right)^2 + \mu_i \left((1+\epsilon_i)|\chi_i|^2 - |\chi_{i+1}|^2 \right) \\ \leq & \mu_i \left((1+\epsilon_i)|\chi_i|^2 - |\chi_{i+1}|^2 \right) \qquad \text{(C-11)}\end{aligned}$$

The evolution of U_i during transmission and receiving instants is evaluated is now evaluated.

We start with the case of a transmission instant, i.e. when vehicle i sends a new measurement. During transmission instants $\tau_i > \tau_{miet_i}$, $e_{u_i} = 0$, using Eq. (3-19) and Eq. (3-21).

$$\begin{aligned} U_i(\xi^+) - U_i(\xi) =& (V(\tilde{x}_i) + \eta_i + \gamma_1\phi_1(0)W_i^2(0) - \\ & \Big(V(\tilde{x}_i) + \eta_i + \gamma_0\phi_0(\tau_i)W_i^2(e_{u_i})\Big) \\ =& \gamma_1\phi_1(0)0 - \gamma_0\phi_0(\tau_i)W_i^2(e_{u_i}) \\ =& (-\gamma_0\phi_0(\tau_{miet_i}))|e_{u_i}|^2 \end{aligned} \tag{C-12}$$

The evolution of U_i during an update event of vehicle $i+1$, i.e. when vehicle $i+1$ receives the measurement, is considered below. It can only update if $\tau_i > \tau_{mad_i}$. Using Eq. (3-20) and Eq. (3-21).

$$\begin{aligned} U_i(\xi^+) - U_i(\xi) =& (V(\tilde{x}_i) + \eta_i + \gamma_0\phi_0(\tau_i)W_i^2(e_{u_i}) - \\ & (V(\tilde{x}_i) + \eta_i + \gamma_1\phi_1(\tau_i)W_i^2(e_{u_i}) \\ =& (\gamma_0\phi_0(\tau_i) - \gamma_1\phi_1(\tau_i))|e_{u_i}|^2 \end{aligned} \tag{C-13}$$

A non-increase of U_i during transmission and update events needs to be guaranteed, i.e. $U_i(\xi^+) - U_i(\xi) \leq 0$. For Eq. (C-12), and Eq. (C-13), this can be guaranteed by setting the following inequalities.

$$\gamma_0\phi_0(\tau_{miet_i}) \geq 0 \tag{C-14}$$

$$\gamma_0\phi_0(\tau_i) \leq \gamma_1\phi_1(\tau_i) \tag{C-15}$$

From Eq. (C-11), Eq. (C-12), and Eq. (C-13), it can be concluded that the storage function $S_i = \dfrac{U_i}{\mu_i}$ satisfies Eq. (C-1) and Eq. (C-2), as U_i is a positive semi-definite storage function which decays in between events and does not increase during transmission or update events. Therefore, the system defined by Eq. (3-21)-Eq. (3-22) has a finite $\mathcal{L}_2$-gain of $\sqrt{1+\epsilon_i}$ with respect to χ_i as input and χ_{i+1} as output.

Bibliography

[1] *Electric vehicles to be 35% of global new car sales by 2040*, Feb 2016. Available at https://about.bnef.com/blog/electric-vehicles-to-be-35-of-global-new-car-sales-by-2040.

[2] B. van Arem, C. J. G. van Driel, and R. Visser, "The impact of cooperative adaptive cruise control on traffic-flow characteristics," *IEEE Transactions on Intelligent Transportation Systems*, vol. 7, pp. 429–436, Dec 2006.

[3] V. S. Dolk, J. Ploeg, and W. P. M. H. Heemels, "Event-triggered control for string-stable vehicle platooning," *IEEE Transactions on Intelligent Transportation Systems*, vol. 18, no. 12, pp. 3486–3500, 2017.

[4] Y. A. Harfouch, S. Yuan, and S. Baldi, "An adaptive switched control approach to heterogeneous platooning with inter-vehicle communication losses," *IEEE Transactions on Control of Network Systems*, pp. 1–10, Jun 2017.

[5] H. Xing, J. Ploeg, and H. Nijmeijer, "Pade approximation of delays in cacc-controlled string-stable platoons," *Advanced Vehicle Control AVEC 16*, pp. 99–104, Jul 2016.

[6] G. J. L. Naus, R. P. A. Vugts, J. Ploeg, M. J. G. V. D. Molengraft, and M. Steinbuch, "String-stable cacc design and experimental validation: A frequency-domain approach," *IEEE Transactions on Vehicular Technology*, vol. 59, no. 9, pp. 4268–4279, 2010.

[7] J. Ploeg, B. T. M. Scheepers, E. van Nunen, N. van de Wouw, and H. Nijmeijer, "Design and experimental evaluation of cooperative adaptive cruise control," in *2011 14th International IEEE Conference on Intelligent Transportation Systems (ITSC)*, pp. 260–265, Oct 2011.

[8] J. Ploeg, N. van de Wouw, and H. Nijmeijer, "Lp string stability of cascaded systems: Application to vehicle platooning," *IEEE Transactions on Control Systems Technology*, vol. 22, pp. 786–793, March 2014.

[9] P. Tabuada, "Event-triggered real-time scheduling of stabilizing control tasks," *IEEE Transactions on Automatic Control*, vol. 52, pp. 1680–1685, Sep 2007.

[10] R. Postoyan, P. Tabuada, D. Nesic, and A. Anta, "A framework for the event-triggered stabilization of nonlinear systems," *IEEE Transactions on Automatic Control*, vol. 60, pp. 982–996, April 2015.

[11] M. Mazo and P. Tabuada, "On event-triggered and self-triggered control over sensor/actuator networks," *2008 47th IEEE Conference on Decision and Control*, Dec 2008.

[12] W. Heemels, K. Johansson, and P. Tabuada, "An introduction to event-triggered and self-triggered control," *2012 IEEE 51st IEEE Conference on Decision and Control (CDC)*, 2012.

[13] Y. Wei, W. Liyuan, and G. G. Dalian, "Even-triggered cooperative adaptive cruise control of vehicles with lumped and time-varying delay," in *2017 36th Chinese Control Conference (CCC)*, pp. 4768–4773, July 2017.

[14] S. Linsenmayer, D. V. Dimarogonas, and F. Allgower, "Event-based vehicle coordination using nonlinear unidirectional controllers," *IEEE Transactions on Control of Network Systems*, vol. PP, no. 99, pp. 1–10, 2017.

[15] S. E. Li, Y. Zheng, K. Li, Y. Wu, J. K. Hedrick, F. Gao, and H. Zhang, "Dynamical modeling and distributed control of connected and automated vehicles: Challenges and opportunities," *IEEE Intelligent Transportation Systems Magazine*, vol. 9, no. 3, pp. 46–58, 2017.

[16] S. S. Stankovic, M. J. Stanojevic, and D. D. Siljak, "Decentralized overlapping control of a platoon of vehicles," *IEEE Transactions on Control Systems Technology*, vol. 8, pp. 816–832, Sept 2000.

[17] S. Sheikholeslam and C. A. Desoer, "Longitudinal control of a platoon of vehicles with no communication of lead vehicle information: a system level study," *IEEE Transactions on Vehicular Technology*, vol. 42, pp. 546–554, Nov 1993.

[18] J. Ploeg, D. P. Shukla, N. van de Wouw, and H. Nijmeijer, "Controller synthesis for string stability of vehicle platoons," *IEEE Transactions on Intelligent Transportation Systems*, vol. 15, pp. 854–865, April 2014.

[19] S. Oncu, N. V. D. Wouw, W. P. M. H. Heemels, and H. Nijmeijer, "String stability of interconnected vehicles under communication constraints," *2012 IEEE 51st IEEE Conference on Decision and Control (CDC)*, 2012.

[20] A. Megretski, "MIT Department of Electrical Engineering and Computer Science 6.242, Lecture Notes: L2 gains and system approximation quality," 2004. Available at "http://web.mit.edu/6.242/www/images/lec3_6242_2004.pdf.

[21] V. S. Dolk, D. P. Borgers, and W. P. M. H. Heemels, "Output-based and decentralized dynamic event-triggered control with guaranteed $\mathcal{L}_p$- gain performance and zeno-freeness," *IEEE Transactions on Automatic Control*, vol. 62, pp. 34–49, Jan 2017.

[22] H. Khalil, *Nonlinear Systems*. Pearson Education, Prentice Hall, 2002.

[23] J. F. Sturm, "Using sedumi 1.02, a matlab toolbox for optimization over symmetric cones," in *Optimization Methods and Software*, vol. 11-12, pp. 625–653, 1999.

[24] J. Löfberg, "Yalmip : A toolbox for modeling and optimization in matlab," in *In Proceedings of the CACSD Conference*, (Taipei, Taiwan), 2004.

[25] F. A. Mullakkal-Babu, M. Wang, B. van Arem, and R. Happee, "Design and analysis of full range adaptive cruise control with integrated collision a voidance strategy," in *2016 IEEE 19th International Conference on Intelligent Transportation Systems (ITSC)*, pp. 308–315, Nov 2016.

[26] R. Goebel, R. Sanfelice, and A. Teel, "Hybrid dynamical systems," *IEEE Control Systems*, vol. 29, pp. 28–93, Apr 2009.

Glossary

List of Acronyms

CACC	Cooperative Adaptive Cruise Control
ACC	Adaptive Cruise Control
V2V	Vehicle-To-Vehicle
V2I	Vehicle-To-Infrastructure
ETC	Event-Triggered Control
TTC	Time-Triggered Control